AD-A107 919 NAVAL RESEARCH LAB WASHINGTON DC F/G 8/3
UNDERWATER FLOW VISUALIZATION METHODS IN THE UPPER LAYER OF THE--ETC(U)
MAY 81 J R MCGRATH, C M GORDON, D GREENEWALT
UNCLASSIFIED NRL-MR-4509 NL

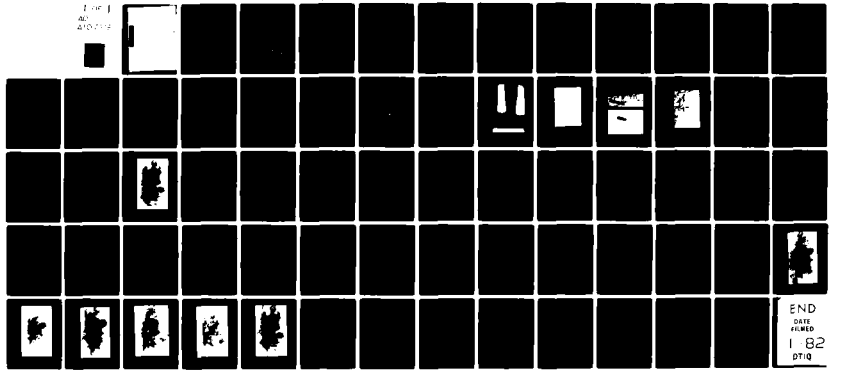

END
DATE FILMED
1 82
DTIC

(12) 67

SECURITY CLASSIFICATION OF THIS PAGE (When Data Entered)

REPORT DOCUMENTATION PAGE	READ INSTRUCTIONS BEFORE COMPLETING FORM
1. REPORT NUMBER NRL Memorandum Report 4509 AD-A107919	2. GOVT ACCESSION NO. / 3. RECIPIENT'S CATALOG NUMBER
4. TITLE (and Subtitle) UNDERWATER FLOW VISUALIZATION METHODS IN THE UPPER LAYER OF THE OCEAN	5. TYPE OF REPORT & PERIOD COVERED Interim report on a continuing NRL problem. 6. PERFORMING ORG. REPORT NUMBER
7. AUTHOR(s) J. R. McGrath, C. M. Gordon, D. Greenewalt, A. Shuetz, C. F. Dohne*, and M. Long	8. CONTRACT OR GRANT NUMBER(s)
9. PERFORMING ORGANIZATION NAME AND ADDRESS Naval Research Laboratory Washington, DC 20375	10. PROGRAM ELEMENT, PROJECT, TASK AREA & WORK UNIT NUMBERS 61153N; RR031-04-41; 43-1324-0-1
11. CONTROLLING OFFICE NAME AND ADDRESS	12. REPORT DATE May 22, 1981 13. NUMBER OF PAGES 66
14. MONITORING AGENCY NAME & ADDRESS(if different from Controlling Office)	15. SECURITY CLASS. (of this report) UNCLASSIFIED 15a. DECLASSIFICATION/DOWNGRADING SCHEDULE

16. DISTRIBUTION STATEMENT (of this Report)

Approved for public release; distribution unlimited.

17. DISTRIBUTION STATEMENT (of the abstract entered in Block 20, if different from Report)

18. SUPPLEMENTARY NOTES

*Present address: Science Applications, Inc., McLean, VA 22102

19. KEY WORDS (Continue on reverse side if necessary and identify by block number)

Flow visualization
Dye tracing
Underwater photography
Measurement technique
Oceanographic instrumentation

20. ABSTRACT (Continue on reverse side if necessary and identify by block number)

A unique approach to measuring shear in the ocean has been developed. The approach involves dye tracing to determine the presence and location of shear in water velocity profiles and underwater photography as the data acquisition technique. Subsequent application of photogrammetric techniques is shown to be feasible and puts the observations on a quantitative footing. The advantage of underwater flow visualization over

(Continues)

DD FORM 1 JAN 73 1473 EDITION OF 1 NOV 65 IS OBSOLETE
S/N 0102-014-6601

SECURITY CLASSIFICATION OF THIS PAGE (When Data Entered)

20. ABSTRACT (Continued)

conventional (free-fall) shear measurements is that the result provides graphic evidence of fluid motion and its subsequent evolution. This approach should lend itself to both new and/or improved models of the upper ocean.

CONTENTS

UNDERWATER FLOW VISUALIZATION METHODS IN THE UPPER LAYER OF THE OCEAN

I. INTRODUCTION

a) Purpose

This report documents the results and status of the Flow Visualization Program formally established under NRL Project 43-1324 in October 1980. In addition to describing methods, equipment and results, the report also discusses advantages and limitations of the approach and recommendations for future developments. This report summarizes results from field experiments conducted prior to and shortly after the formal establishment of the project.

b) Scope

As a result of recent experience, a field exercise was conducted in Key West during 14 - 22 August 1980 to obtain synchronized stereophotographic records. Several secondary objectives were also identified. First, dye sheets were dispensed above, at and below the diurnal thermocline. Second, various equipment tests were conducted under operational conditions; these tests concerned: a method to trigger shutters and to advance film simultaneously on three underwater still cameras; a temperature-difference sensor to determine density difference between dye plumes and surrounding water; a computerized weather station and a new wavestaff design. Finally, the upper ocean hydrographic structure was measured using CTD and XBT equipment.

The operations area is shown in Figure 1. The Key West site was chosen because the NADC Detachment provided outstanding support and because underwater visibility in that area is very good. The field measurements took place just south of the sea buoy marking the Main Ship Channel. Operations took place in water depths of 100 ft, located approximately 12 nm south of Key West.

II. BACKGROUND

a) Project Objective

The principal objective of this project is to identify and characterize transport mechanisms in the upper ocean and to establish their temporal and spatial properties. To achieve this objective, underwater photography is the primary data acquisition system. After having identified and characterized transport mechanisms in the upper ocean and having established their temporal and spatial properties, the principal program objective is to validate major aspects of existing models, to stimulate their subsequent improvement, and, where appropriate, to promote the development of new models.

b) Previous NRL Efforts/Exercises

The Physical Oceanography Branch, Naval Research Laboratory (NRL), has previously conducted three exploratory tests in its approach to underwater flow visualization. The first, during July 1979, took place near Bermuda and

Manuscript submitted March 10, 1981.

involved the testing of both vertical and horizontal dye dispensing techniques. Vertical dye dispensing was achieved using dye bombs, XBT bodies filled with solid-dye pellets. Horizontal dispensing was achieved using a "T-bar" deployed at or near the bottom of the mixed layer, usually 20 to 40 ft deep. This system used liquid dye.

The second test took place during the Branch cruise 150 nm south of Bermuda during September - October 1979 with improved results. In this exercise, however, the "T-bar" proved difficult to position at desired depths because of ship- and surface-induced motions.

The third test was conducted off the southern coast of the island of Vieques near Puerto Rico during 16 - 25 April 1980. The test objective, stabilizing the "T-bar" at specified positions in the water column, was achieved. This result paved the way for the following field exercise. Its objective was to determine hydrographic and meteorological conditions at the observation site and to relate these conditions to photographic observations of underwater dye dispersion.

As might be surmised, these pilot efforts were necessary not only to determine the experiment's equipment and personnel requirements, but also to develop the necessary skill and experience in manipulating these components in an at-sea environment.

c) Motivation

Historically, measurements of oceanic motions have employed moored current meters. These provide long-term measurements of currents at fixed depths. Such time-series data, however, yield little insight into the spatial and temporal variations of sub-surface fluid motions related to turbulence, shear, coplanar flows and surface waves. As a result, neither the forces stirring the upper ocean nor their complex inter-relationships are well understood presently.

In recent years, increasing attention has been given to the uppermost layer of the ocean, largely because of its relevance to air-sea interactions. McGrath and Osborne (1) for example, describe the influence of near-surface oceanic motions which partly contribute to the difficulty of interpreting infrared images of the sea surface. Garrett's (2,3) studies indicate that the formation and maintenance of surface slicks are notably affected by sub-surface fluid motions, e.g. Langmuir cells, turbulence and upwelling. These are but two examples illustrating why the uppermost oceanic layer stimulates scientific interest.

In studying this region, highly specialized instrumentation and techniques have been developed. These have usually taken the form of free-fall bodies equipped with fast-response sensors. Osborn's (4) instrument, for instance, measures velocity shear and temperature to depths as great as 200 m. While this approach has provided useful information, it yields an instantaneous view and, as yet, only suggests what forces and mechanisms dominate at that moment. Nonetheless, a growing amount of information is being accumulated about the ocean's microstructure. A most revealing approach to studying upper

oceanic fluid motions has been undertaken by Woods (5). He used dye and underwater photography near Malta to trace the water's motion. His approach provided graphic evidence of thin laminar flow sheets spaced about 4 m apart. To summarize Wood's findings, the thermocline between 0 and 50 m reveals a fine structure consisting of about a half dozen layers of low shear and moderate temperature gradient separated by thin laminar flow sheets with markedly increased shear and temperature gradient.

The employment of dye both to visualize and to measure fluid flow phenomena in the upper ocean is attractive for several reasons. First, the visualized phenomena lend themselves to modeling. Second, dye provides a significantly longer period of observation than free-fall instrumentation. The period not only increases the data base but may also provide a more complete understanding of the observed phenomena than does free-fall instrumentation. Finally, employment of dye to trace subsurface flow patterns is analogous to flow visualization techniques used in wind tunnels. These have provided invaluable insights into processes which otherwise could often be studied only by indirect techniques. For these reasons, flow visualization offers the promise of increased understanding of upper ocean phenomena and of their relative contributions to development of the mixed layer and vertical transport of heat, salt and momentum.

III. EXPERIMENTAL ARRANGEMENT

a) General

Operations at sea have been conducted from a patrol boat, landing craft and from a large research vessel (USNS LYNCH). Of these, the most suitable platform was the landing craft. It not only accommodated the scientific party (12 people), but also greatly facilitated diving operations. The activities involved in conducting at-sea operations are outlined in Figure 2.

Environmental observations are made to assist in on-site decisions affecting operations and to provide information needed in the subsequent data analysis. Of considerable importance is the determination of the mixed layer depth using temperature structure as the primary indicator. Both XBT and CTD measurements are made for this purpose. Meteorological data (wind speed, wind direction and barometric pressure) are recorded continuously while the vessel's drift rate and local wave heights are measured periodically using a log and wave staff, respectively.

Execution of the experiment involves deploying the "T-bar" as a spar buoy at depth and decoupling it from surface-induced motions using the wave staff and variable flotation. Once dye is being dispensed from the "T-bar", dye bombs are dropped through the resulting dye sheet to determine the presence and magnitude of shear currents above, at or below the mixed layer. Working divers adjust the equipment under water, while underwater photographers use still and motion picture cameras to record events. Because the platform cannot be underway during these operations, a diver support boat is always provided to assist the divers and to drop the dye bombs.

This section addresses specific details of the equipment.

b) Dye Injection System

A dye - sea water mixture is pumped to the selected depths producing a horizontal dye sheet. The dye injection system consists of main and auxilary metering pumps, a double, non-collapsable rubber hose, a perforated "T-bar" dispenser and two types of buoyant suspension systems.

The main pump is a flexible-impeller, positive displacement pump (Cole-Parmer Model 7093). It draws sea water from the dye-dispensing depth through the intake hose to the support vessel. There, the sea water is mixed with dye and pumped through the return hose to the desired dispensing depth at a nominal rate of 11 gallons per minute (gpm). The auxiliary metering pump (Fluid Metering Inc. Model RP-D-1CSC) injects the dye at a rate of about 0.12 gpm and provides a dilution ratio varying between 10^{-2} to 10^{-3}. The dye is a yellow-green, water-soluble fluorescent liquid concentrate (Horizon Ecology Co., Cat. No. 298-07). The concentrate is fed directly into the auxiliary metering pump. The hose is a non-collapsable type, 0.75-inch inside diameter.

The "T-bar" is attached to the end of the output hose and is a surface-supplied tube. It dispenses the dye sheet at any desired depth in the water column. The "T-bar" is a 0.50-inch diameter copper tube having 0.25-inch diameter holes drilled at 2.25-inch intervals along its entire 10-ft span.

Because the hose directly connects the "T-bar" to the surface ship, two methods of supporting and decoupling the "T-bar" are employed. The first is a spar buoy, which is also used separately as a wave staff. When the "T-bar" hose is suspended from the spar buoy, much of the wave-induced ship motion is suppressed.

The effects of these motions are almost entirely eliminated when the second suspension system is utilized. This system consists of a weight (lead brick) and one or more inflatable bags (BUWEPS, Mk 138 Mod 1). Divers inflate the bags as needed to provide depth adjustments yielding the desired "T-bar" depth and neutral buoyancy. Both the weight and the bags are attached at the mid-point of the "T-bar's" span. The dye-dispending depth, weight of the lead brick and the amount of hose at and near the "T-bar" determine the extent to which the bags are inflated.

c) ΔT System

The intake and output hoses are at approximately the same depth when the dye injection system is operating. Experience and measurement indicate that a temperature difference between intake and output hoses can be as large as 0.10°C. Both mechanical pumping action and solar heating of hoses on deck contribute to this temperature difference. Such a temperature difference can cause artificially buoyant dye sheets which are not true Lagrangian tracers of near-surface water motions. To eliminate artificial buoyancy in the dye sheets, two steps have been taken.

The first step is to monitor continuously the temperature difference between the intake and output hoses. The ΔT system, constructed for that

purpose and shown schematically in Figure 3, is essentially a bridge circuit balancing the outputs of two thermistors. One thermistor is located in the base of the "T-bar" (output hose) and one is located at the entrance of the intake hose. Two Fenwal Electronics Thermistors (GB41P2) are the main components of the ΔT system. These are potted in 0.625-inch copper tubes and are connected to the bridge network using 100 ft of rubber-covered, shielded cable. The cable is grounded on the instrument end. An ammeter records the temperature difference, and, with the aid of a digital voltmeter, provides a thermal resolution of $0.05^{o}C$. In operation, the thermistors are lowered to the desired depth for about 15 minutes, where they are allowed to reach thermal equilibrium with the ammeter power on. The ammeter is then set to zero and the system is ready for operation.

The second step taken to eliminate artificial buoyancy in the dye sheets is to adjust the voltmeter to zero by moving the intake hose deeper into the water column. This adjustment is predicated on two assumptions. The first assumption is that a sufficient temperature gradient exists over the range of the "T-bar" operating depths. This condition permits the intake of slightly cooler water which compensates for the unavoidable heating of seawater due to pumping and to solar influences. The second assumption is that salinity remains constant over the depth variations of the water hose. As a result, the ΔT system gives continuous quantitative information concerning the temperature difference between the intake water temperature and the sea water - dye mixture temperature.

d) Dye Bombs

To determine the horizontal shearing motion of the water mass above, at and just below the dye sheet, dye bombs are dropped through the dye sheet from a small surface support boat. The dye bombs are made from XBT bodies filled with four to six yellow-green fluorescent dye tablets. Both T-11 and T-7 XBT bodies (shown in Figure 4), have been used to provide observations of water motion. They have nominal descent speeds of 5 and 20 fps, respectively. As the XBT descends, it leaves a dye trail from the water soluble dye tablets (Horizon Ecology Co. Cat. No. 295-07). A photograph showing the dye trail passing through the dye sheet is provided in Figure 5. Motion picture films of the subsequent convolution and dispersal of the dye bomb's trail adjacent to the dye sheet provide a measure of the local influences acting on the dye sheet. In the future, photogrammetric measurements will provide quantitative shear measurements.

e) Support Vessel

The primary support vessel during the Key West exercise was a LCM - 8 landing craft shown in Figure 6. It was operated by the NADC Key West Detachment. The LCM-8 is 76 ft long with a 21 ft beam and easily accommodates a scientific party of 12 to 16. Equipped with four GM 6-71 diesel engines, the LCM-8 cruises at speeds of 8 to 10 kt, making operation areas up to 20 nm away reasonably accessible. To accommodate the NRL equipment needs, a small air-conditioned van was added; the van housed recording and other electronic equipment. Because the bow ramp can be lowered, the LCM-8 is especially well-suited to support diving operations. Both divers and an

inflatable rubber boat utilized the ramp during diving operations. Although a gyro compass is standard, a Loran-C navigation system was also available. Ship-to-shore VHF communications was part of the vessel's equipment.

f) Diving Operations

The Fleet Audiovisual Command and Naval Special Warfare Group Two supported this and three previous flow visualization efforts. Navy and civilian divers in this experiment carried out underwater work assignments and photographed both the dye sheets, as shown in Figure 7, and dye bomb tracks.

SCUBA diving techniques are used to achieve the experiment's objectives. All diving operations are under the control of a Diving Officer and are conducted in accordance with the US Navy Diving Manual. All divers are Navy-trained, holding current certification in this specialty. Swimmers participating in these operations are currently-qualified First-Class Navy swimmers.

The primary role of the scientist-diver is to supervise the underwater work and to make in-situ technical observations. Only limited time exists during any SCUBA dive to carry out the work plan. Because the total group at sea is of such diverse background (scientists, combat swimmers, underwater photographers and ship's crew), the approach using a scientist diver to supervise underwater activities assures the highest likelihood of success in proceeding from work plans to executed assignments under water.

g) Underwater Photography

Two camera systems were used in the underwater photography. The first system was a Milliken* DBM9-1 motion picture camera. This hand-held, electrically-driven motion picture camera operated at 24 frames/sec. Equipped with a 6.6 mm, water-contact lens (corrected for underwater distortion), the total field of view was 76°.

The second system consisted of three Nikonus III cameras that provided still underwater photography, the major data acquisition technique. The Nikonus III had a 15 mm lens, giving a 90° total field of view. With Ecktachrome 35 mm color film (ASA 200), shutter speeds of 1/125 sec were typical for prevailing underwater light conditions. In order to get three-dimensional information on both the dye sheet and vertical dye tracks, a "stereoscopic" photographic system was developed.

The stereoscopic design involved a rigid bar on which the three cameras were mounted; each camera was separated by 1 meter. The end cameras were aimed inward at an angle of 20°, so that all three photographs would overlap for an object distance of 2.8 m. The design permitted all three camera shutters to be manually triggered simultaneously. The design also provided simultaneous film advance and shutter cocking for the three cameras. This method was intended to simplify the underwater operation of the camera bar and to allow rapid photographic sequences to be taken if required. A 1 m-long

*Teledyne Camera Systems, 131 No. 5th Ave., Arcadia, CA 91006, now produces the Milliken camera.

rod projecting normal from the center of the camera bar provided a reference point for the three photographs. At the end of this rod was mounted a clock, depth gauge and plumb bob, within the field of view of all three cameras. Rotation during a sequence of any camera with respect to the bar was detectable by means of this reference point. The watch showed hours and minutes in analog form and the date and seconds in liquid crystal display. The watch was to provide a unique label for each frame on each of the three films, showed time interval between pictures in a sequence and indicated gross asynchronism of shutter triggering. The depth gauge and plumb bob gave further information on bar position and orientation in the water column. Wide angle (28 mm) lenses were used later on the cameras to reduce the distance between subject and camera, and thus minimize haze due to particles in the water. Styrofoam flotation was added to the bar to make it neutrally buoyant.

Operation of the prototype 3-camera system proved difficult for several reasons. First, the triggering mechanism was found to be unreliable and had to be discarded. In its place, a second diver operated one camera, while the first diver operated the other two. Second, the wristwatch was readable only in some of the photographs of the central camera and then only in its analog display. Thus, time information of less than a minute was not resolvable. Nevertheless, picture quality was good. The time interval between photographs in a sequence was estimated to be as little as 10 sec, and the divers reported that they could synchronize pictures to considerably less than 1 sec. Care was taken to keep the three films from each photographic sequence in order throughout development. Thus, except for the need of an extra diver, operation of the camera bar was satisfactory. Redesigning of the 3-camera system is in progress.

h) Environmental Equipment

Of the five instruments yielding environmental data, two instruments provide hydrographic data. The first instrument is the Sippican Expendable Bathythermograph (XBT) System. The components of this system include the recorder (Mk 2A-1), launcher (LM 3A), XBTs (Model T-11), and Test Set (Model A-4). This equipment is described in detail in Reference 6. Examples of XBT data are given and discussed subsequently in this report.

The second instrument is a Martek Instruments Inc. Metering System (Model CTD).* It consists of a solid-state read-out module, a multi-conductor underwater cable with molded connection and a remote multielement sensor package. The latter contains a thermistor temperature transducer, a diffused silicon diaphragm pressure transducer, and a platinized conductivity cell. The instrument is portable (battery operated) and is equipped with 100 ft of cable; the sensor package is manually lowered into the water. The CTD data serves two purposes. First, it provides an alternate means of determining the temperature structure of the water column and serves generally to confirm XBT data. Second, the CTD provides salinity data which serves to validate a priori assumptions concerning salinity variations within the uppermost portion of the water column. Details concerning the operation of the CTD are contained in Reference 7. Examples of CTD data are given subsequently in this report.

*Martek Instruments Inc., 17302 Daimler Street, PO Box 16487, Irvine CA 92713

The third instrument is a small weather station (Heathkit Model IDW-4001) which provided meteorological data during the course of the underwater measurements. In addition to its digital time capability, the weather station gives wind speed and direction, barometric pressure and inside and outdoor temperature. Equipped with a microprocessor, the unit stores maximum and minimum barometric pressures and temperatures, in addition to peak and average wind speeds. All data are digitally displayed and manually recorded. An example of weather data obtained during 21 August 1980 is given in Figure 10.

The fourth instrument, a log and line, is aptly suited to this experiment and measures the ship's drift speed relative to the local surface water (rather than ship speed relative to the earth). Written description of the use of log and line to determine ship speed appeared probably for the first time in William Bourne's "A Regimen for the Sea" (1574), Reference 8, although the method had likely been in use well before that date.

> *'To know the ship's way* [writes Bourne] *some do use this, which (as I take it) is very good: they have a piece of wood, and a line to vere out over boorde, with a small i.e. thin line of a great length, which they make fast at one ende, and at the other ende, and middle, they have a piece of lyne which they make fast with a small thred to stande lyke unto a crowfoote: for this purpose that it should drive asterne as fast as the shippe doth go away from it, always having the line so ready, that it goeth out as fast as the ship goeth. In like manner they have either a minute of an hour glass, or else a knowne parte of an houre by some number of woordes, or such other lyke, so that the line being vered out, and stopped just with that tyme that the glasse is out, or the number of wordes spoken, which done they hale in the logge or piece of wood again, and looke how many fathomes the shippe hath gone in that time.'*

The log used in this experiment consisted of an aluminum sheet 30 x 40 cm, buoyed at one edge with a strip of styrofoam. The log floated vertically in the water; its upper edge protruded less than 1 cm above the surface. Wind drag, therefore, had very small effect on the log. Knots were employed in the NRL log, spaced at half-meter intervals over a line length of 12 meters as a measure of line payed out. Time was measured with a quartz crystal-controlled stopwatch. Otherwise, the measurement differed little from the technique Bourne described above.

The fifth instrument is a wave staff to provide wave height measurements at the time and site of dye deployment. The wave staff is a long, thin and weighted spar buoy equipped with a damper plate suspended some distance below. As a consequence, the wave staff's vertical motion is relatively unaffected by vertical water motion associated with the surface waves. Since the buoy is assumed to be vertically stationary, wave height is measured by the relative travel of the water surface up and down its vertical extent. It should be clear that only short period waves could be measured with the wave staff as shown in Figure 8.

The spar buoy was made from PVC tube, 11.4 cm diameter and 305 cm long, filled with a self-expending and hardening foam (ISOFOAM - PE2). In air, it weighed 3.5 kg and displaced 31 kg water. Lead weights of 18 kg were suspended from the buoy's bottom and caused it to float vertically with about 1 m above the average water surface. The buoy's natural period was computed to be 2.8 sec. The damper plate, a circular disc 40 cm in diameter, was suspended with flat surface horizontal, 5 m below the buoy. Observation in calm water showed that the system was critically damped. At the top of the buoy, six stripes of different colors, each 25 cm wide, had been painted. This allowed quantitative visual measurement of wave height, which was recorded on motion picture film during each day's operation.

The same spar buoy was also used subsequently to decouple the "T-bar" from surface wave motion. In previous flow-visualization experiments, the "T-bar" moved vertically due to wave motion. This motion occured either when the suspended hoses directly coupled the "T-bar" to the boat or when a surface float of 30 cm diameter supported the "T'bar" near its attachment. The "T-bar" motion produced a horizontally undulating dye sheet. Use of the small diameter spar buoy as a support for the "T-bar" provided a great improvement in the vertical stability of the latter, so that the dye sheet was observed to be quite flat at all dispensing depths.

An additional method of recording wave motion using the spar buoy made use of seven wire rings spaced at 25 cm intervals on the upper end of the buoy. Each ring is connected through a resistor to an oscillator circuit within the buoy. The resistor circuit, shown in Figure 9, is arranged to cause the lowest ring to short successively to each ring above it, and the oscillator frequency to increase progressively in units of 1/3 octave. With all resistors over 70 kΩ, a sea-water contact between rings is essentially a short circuit, so that when the buoy is properly arranged at sea, the oscillator frequency is a step-wise measure of wave height. The coaxial cable connects the oscillator output to a cassette recorder on the boat. Subsequent playback of the cassette through a frequency counter and D-A converter onto a strip chart recorder produces an interpretable record of wave motion. Due to a battery failure in the sealed oscillator circuit, this system was not used during the experiment.

IV. DISCUSSION

a) Environmental Analysis

Photographic data obtained during Thursday morning, 21 August 1980, were selected for processing and analysis; this section, consequently, concerns only those supporting observations of that period. The general schedule of events that morning are listed below in Table 1.

Table 1

LOCAL TIME	COMMENTS
1040L	Divers in the water
1107L	Depth: 35 ft; 80 sec of dye dispensed
1113L	Depth: 30 ft; 60 sec of dye dispensed
1120L	Depth: 25 ft; 90 sec of dye dispensed
1125L	Divers and swimmers out of water

Meteorological data are summarized in Figure 10, which gives wind speed, wind direction and barometric pressure as the ordinates and local time (on a 24-hour basis) as the abscissa. The barometric pressure showed a steady increase, 0.00133" of Hg/min, rising from 29.74" of Hg at 1030 L* to 29.82" at 1130L. Wind speed was averaged over 10-min. intervals and during morning operations did not exceed 7.5 kts. Wind direction was very consistent and fluctuated no more than 10° from its average direction, 190°T. Prior to diving operations the sea was calm. The air temperature in the shade on deck was 86° F and at 1018 local time the ship's drift rate was estimated to be 0.079 m/sec.

Hydrographic data consisted of XBT, CTD and wave staff measurements. Casts using T-11 XBTs were made at 1003L, 1153L, 1325L and 1443L. The results of these casts are summarized in Figure 11, where the depth in meters is the ordinate and temperature in °C is the abscissa. The data are terminated at the 50-meter depth, the extent of interest in this experiment. At the 10-meter depth, the mean depth for diving operations during the morning of 21 August, the temperature gradient increased throughout the day and was determined to be 0.154, 0.200, 0.235 and 0.364°C/m. Both temperature measurements throughout the water column and gradient calculations at the 10-meter depth indicate the upper layer was not well mixed that day, in contrast to the previous day. During 21 August, the seasonal mixed layer depth remained very constant at 12 to 14 meters. This result is attributed to the vessel's limited drift and suggests limited spatial horizontal variability in the water.

Both temperature and depth functions of the CTD instrument operated satisfactorily during the experiment, although the salinity function did not. To provide an improved measure of temperature, a calibrated thermistor was taped to the CTD sensor package and a digital voltmeter was used to provide more precise temperature readings. The thermistor had a response time of 0.1 sec and a thermal resolution of 1/500°C. Figure 12 provides both XBT and CTD temperature measurements to the 30-meter depth; these data were taken within 8 minutes of one another. The XBT data agree to within 0.50°C and the XBT

*Local times are designated by the letter L and all directions are magnetic bearings in degrees true (°T).

data trend closely follows the thermistor data trend. At the same depth, comparison shows that XBT data are consistently lower than CTD data. The most probable cause of this behavior is a systematic error in the CTDs depth sensing function.

Bathymetric conditions in the operations area have been shown previously in Figure 1. Operations were conducted south of the outermost sea buoy marking the ships' channel to Key West. Relative bearings to the outermost sea buoy and fathometer* readings confirm that operations were conducted in at least 100 ft of water. Consequently, the conditions of the experiment are considered sufficiently representative of the deep-ocean environment.

b) Photographic Analysis

The Naval Intelligence Support Center (NISC) provided photogrammetric processing and analysis of the 35 mm film from the still-camera arrangement described previously. Films (about 100 frames in all) from the three cameras were supplied to NISC, along with information about the camera's focal length and separation, exposure interval, and camera orientation.

Figure 13 is an enlargement and an example of the photographs subjected to processing. Numbers written on the photograph are points selected for input to the computer for subsequent processing. The computer calculates object space coordinates using three overlapping photographs. Figure 13 is only one of three photographs required for this calculation. The three photographs are taken synchronously and identify the instantaneous position of the dye pattern at a specific moment. For exposure intervals of 5 to 15 seconds, therefore, it is possible to determine the motion of a particular dye pattern feature. Overlapping coverage by all three cameras of the target feature is necessary to satisfy processing requirements. The photogrammetric processing and analysis details are discussed further in Reference 9.

Figure 14 is an outline of the top view of the dye pattern in a similar photograph. To obtain this solution, the position and orientation of the camera station are inputs derived from a previous computer calculation. By overlaying this plot with subsequent plots, the dye's motion can be determined. In examples randomly chosen and separated by 20 sec, movement of 0.07 m is observed. This value is accurate within 0.02 m. The motion of the dye patch during this interval is, therefore, 3.5 mm/sec $\pm$ 1.1 mm/sec. As a general consequence of this analysis, dye tracing in the upper water column is established as a viable means of studying oceanic motions.

c) Recommendations

In this section are given three recommendations based on the lessons learned from previous experiments. In general, the recommendations are to improve the data acquisition technique rather than to purchase new equipment.

*Ross Model 400-A Fineline Fathometer, Ross Laboratories, Inc., Seattle WA.

While the "T-bar" behaves adequately in terms of dispensing relatively flat dye sheets, one modification can improve its present performance and extend the system's capabilities up to sea state 2. This modification involves replacing the lead brick at the "T-bar" with a lead damping plate, It would serve a dual purpose. First, the damping plate provides a suitable weight to be counter-balanced by the inflatable bags. Second, the effect of the damping plate located at the "T-bar" would reduce any vertical excursions of the dye sheet. The damping plate should be located at least 5 ft below the "T-bar" so that the plate's wake will not disturb the dye sheet.

For the measurement of wave height, three improvements should be made to the spar buoy system. During this particular experiment, wave height did not exceed 1.5 m crest-to-trough, however, future experiments may be carried out during conditions of greater wave height, i.e. beyond the present measuring range of the system. Therefore, the buoy height needs to be increased. Second, an increase in the natural period of the spar buoy would allow measurement of longer period waves. This is desirable and can be achieved by increasing the buoy's vertical dimensions. Finally, mounting the wave recorder inside the buoy should be a feature of the wave height recording system, because wave height is best measured with the buoy free-floating, untethered to the ship.

V. SUMMARY

a) General

This report documents the results of an experiment conducted in Key West during 14 - 22 August 1980 to develop, test and validate procedures and methods in support of the Underwater Flow Visualization Project.

The primary experimental objective, using synchronized stereo-photographic records to obtain fluid motion measurements, has been achieved. All secondary experimental objectives have been met. First, dye sheets were dispensed above, at and below the mixed layer depth. Second, equipment tests have been conducted under operational conditions. While all the equipment proved to be generally adequate and compatible for their intended experimental purposes, suggestions are made to improve their contribution to the experiment's results. These improvements involve modifications as contrasted to major equipment purchases. Third, the ocean's upper hydrographic structure has been characterized in support of the experiment's analytic needs. Finally, the diversely-trained personnel have been identified and organized to carry out this experiment.

b) Status

The Underwater Flow Visualization Project has progressed to the point where tested experimental procedures are now established. Underwater photography has been shown to be an effective data acquisition technique. Existing photogrammetric procedures have been employed to provide quantitative information. Four field experiments have been conducted over the past 18 months validating the efficacy of this approach. A reliable technique is now available for the scientific study of horizontal and vertical motions in the deep ocean at depths to 120 ft.

VI. ACKNOWLEDGEMENT

During the Key West experiment, Mr. Dan Probert and Mr. Bill Hartman, the NADC Detachment hosted the NRL scientific party and provided outstanding administrative and material support. A note of appreciation is due the Commanding Officer, Underwater Demolition Team 21, who provided diving personnel. A special note of appreciation is due LT (jg) J. Luksyk USN, MM1 J.D. Redmond USN, QM1 E. Leasure USN and MM3 Kevin Barnes USN for their unreserved efforts and diving expertise. Personnel from the Fleet Audiovisual Command provided the underwater photographers under the direction of PHCS D.J. Graver USN. To these and many others who contributed to this program, the authors are most grateful.

VII. REFERENCES

1. J.R. McGrath and M.F.M. Osborne, J. Phys. Oceanog. 3, 318-327 (1973).
2. W.D. Garrett, Ann. der. Met., N.F. Nr 4, 25-29 (1969).
3. H. Huhnerfuss and W.D. Garrett, J. Geophys. Res. 86, 439-447 (1981).
4. T.R. Osborn, Man. Rept 31, Inst. of Oceanogr. Univ. of British Columbia, Vancouver (1977).
5. J.D. Woods, J. Fluid Mech. 32, 791-800 (1968).
6. Anon., Sippican Instruction Manuals, R603 and R662.
7. Anon., Maetek Instruction Manual, Part No. 101-S.
8. E.G.R. Taylor, The Haven-Finding Art, William Bourne, A Regimen for the Sea, American, Elsevier Pub. Co., New York, pg. 201 (1971).
9. Mensuration of Underwater Photography Using Photogrammetric Techniques, prepared by Naval Intelligence Support Center, Suitland, MD for Naval Research Laboratory, Enclosure (1) to Ser 74/7269 dtd 28 Nov 80.

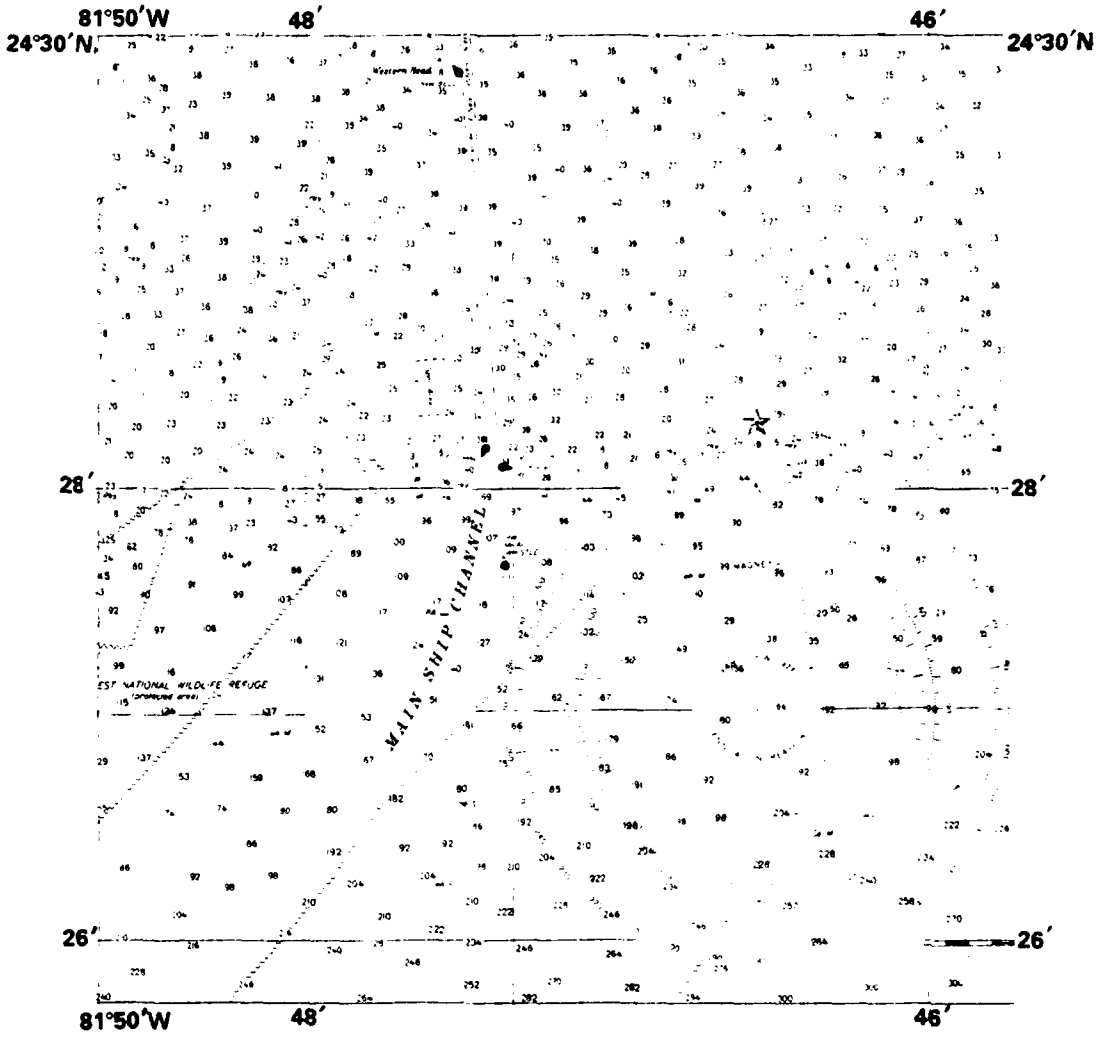

Fig. 1 — Chart of the Operations Area; soundings are in feet

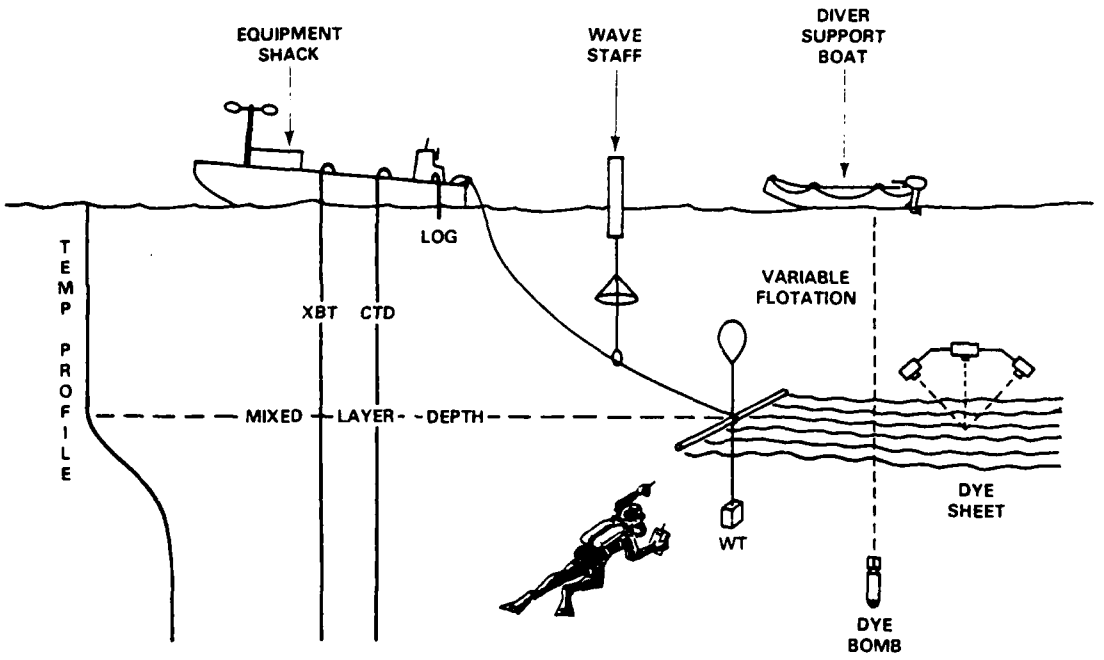

Fig. 2 — Experimental arrangement

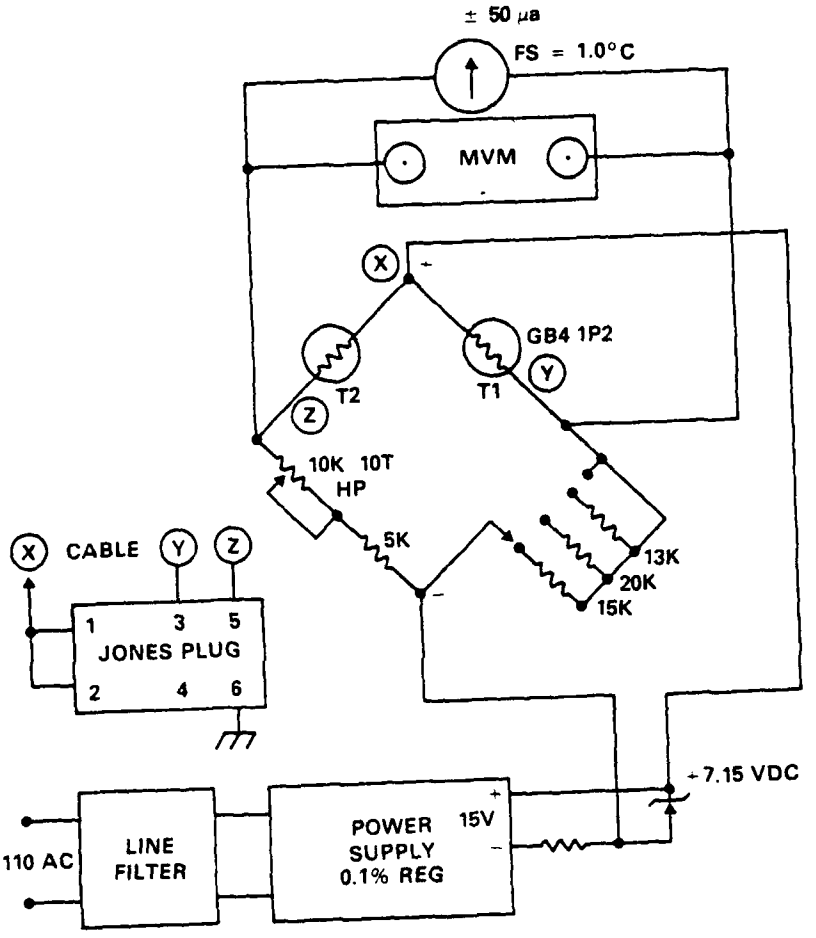

Fig. 3 — Schematic of the ΔT system

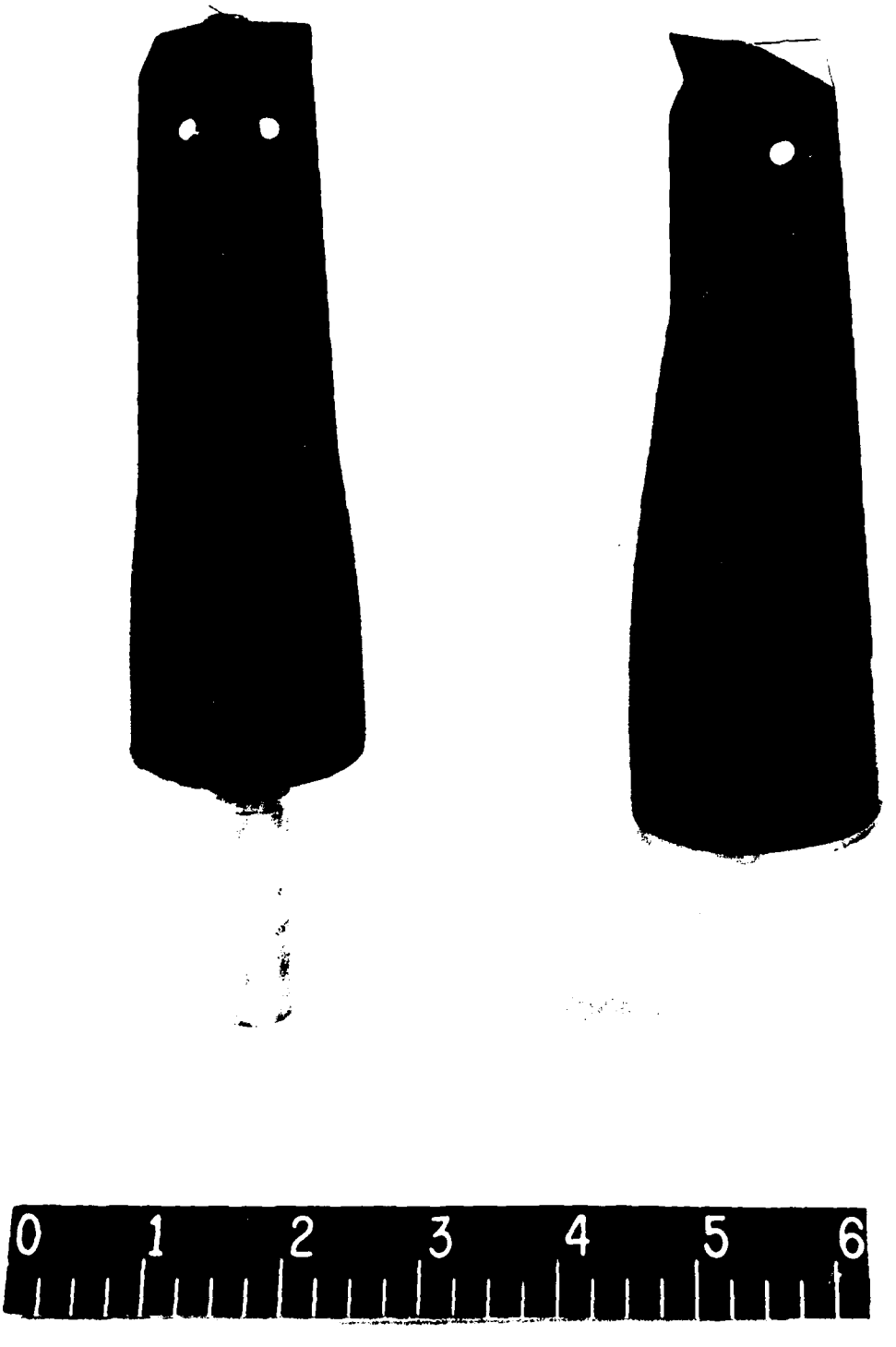

79512(1)

Fig. 4 — XBT-11 and -7 bodies used as dye bombs

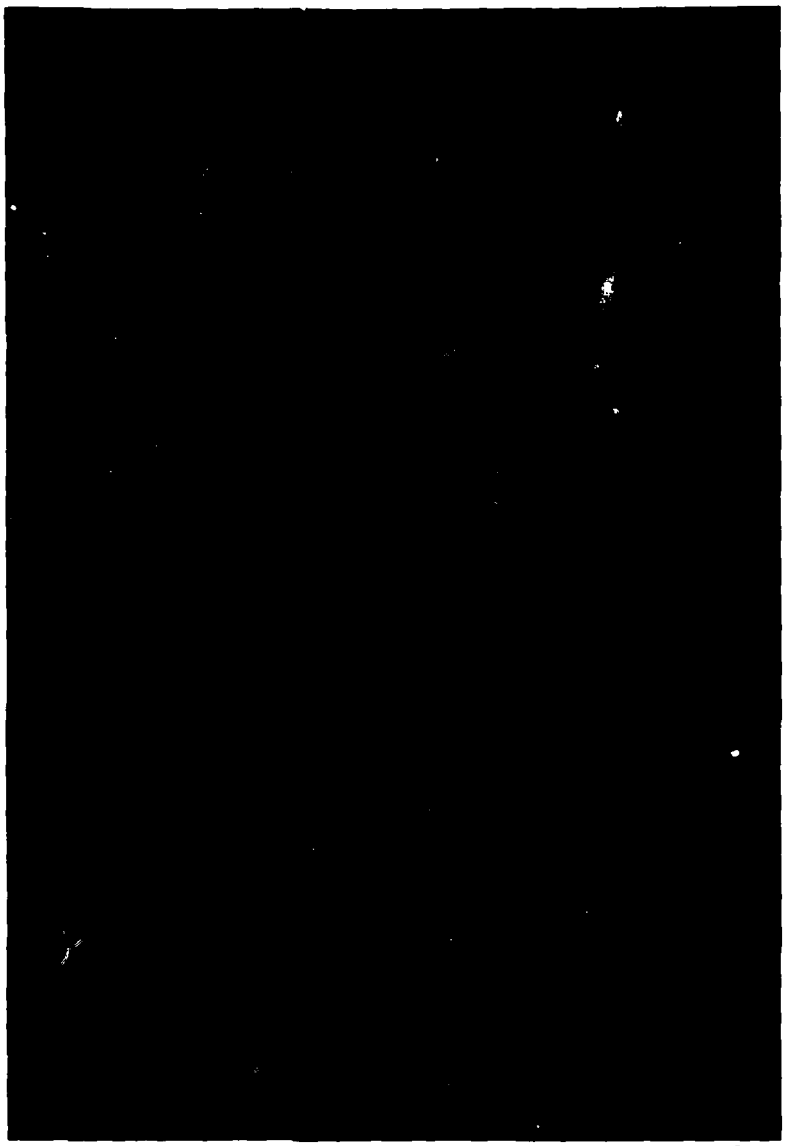

R-021

Fig. 5 — Generation of a dye trail in the water column

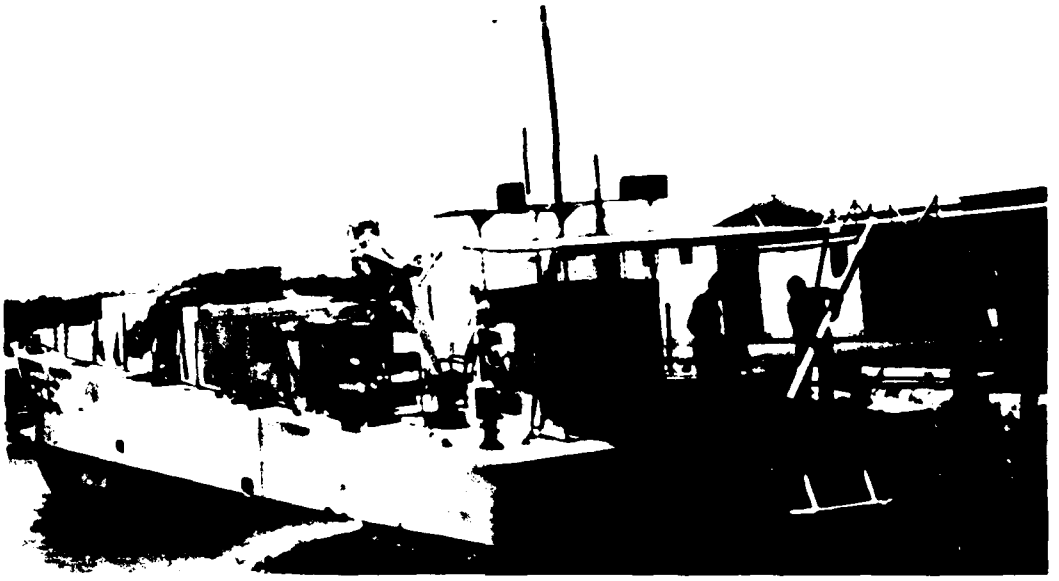

R-023

R-023

Fig. 7 — Dye sheet generated from the "T-bar"

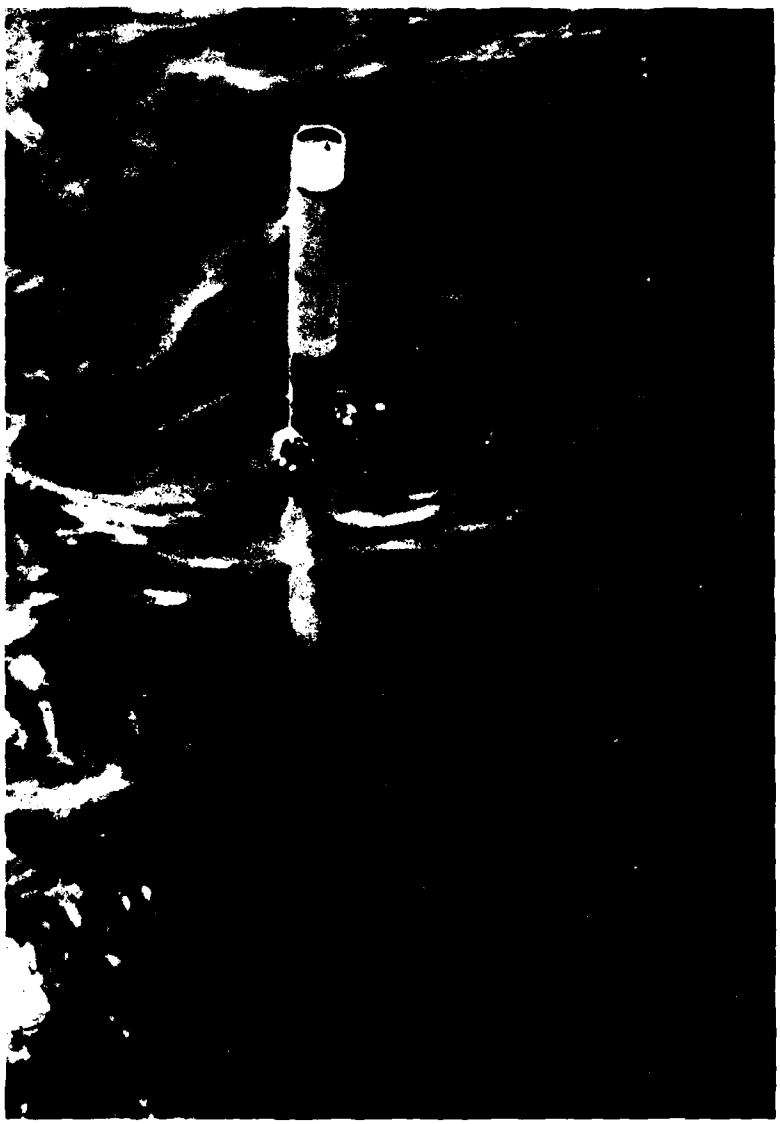

R-022

Fig. 8 — Wave staff

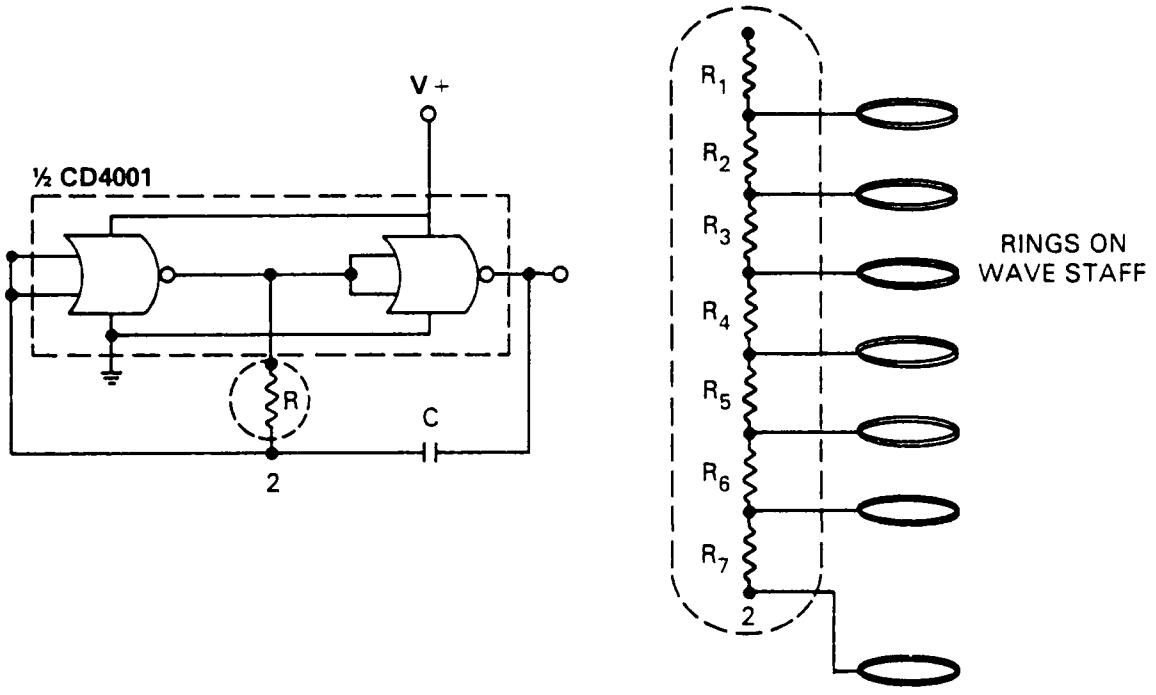

Fig. 9 — Schematic of the wave staff resistor circuit

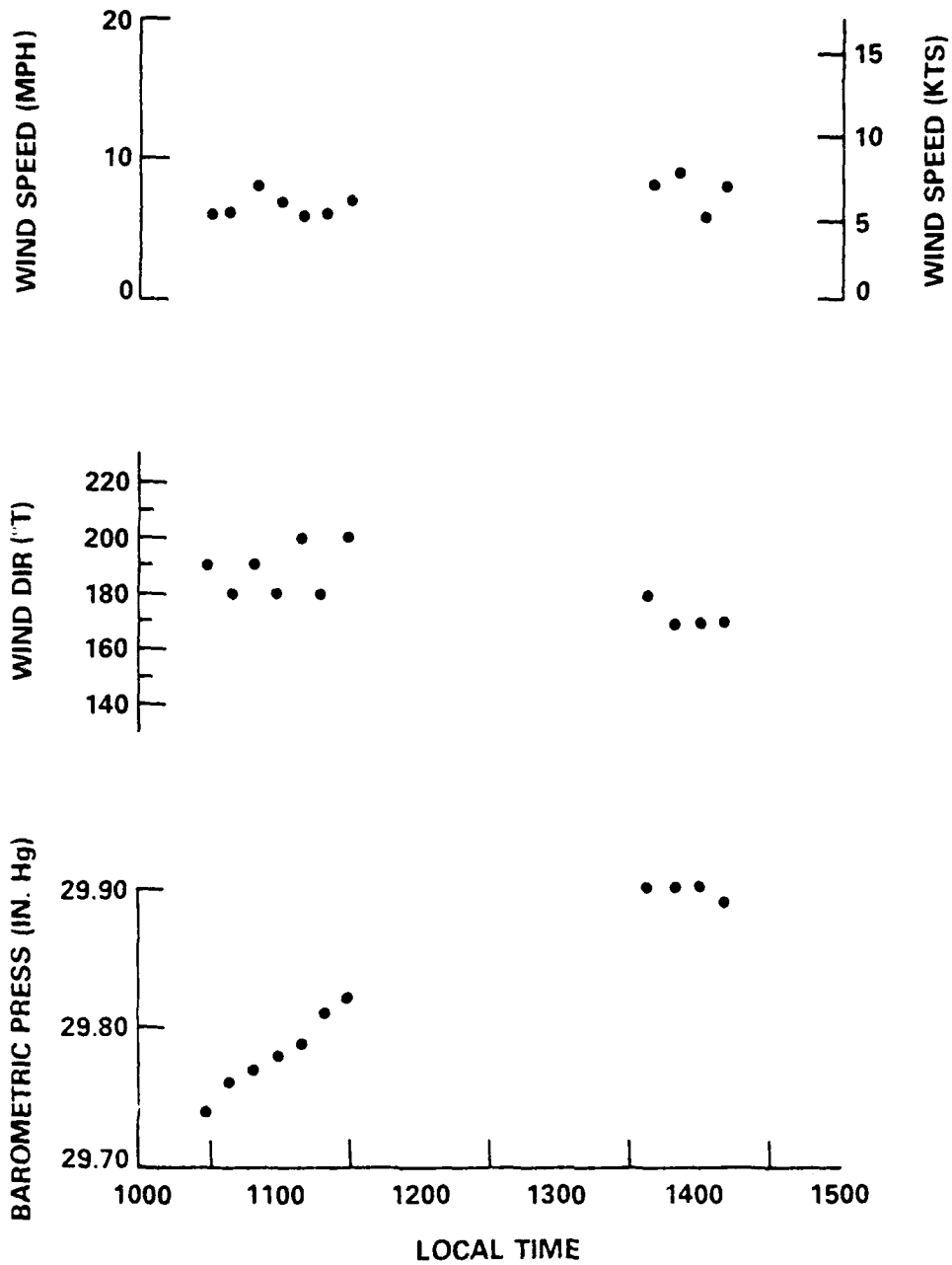

Fig. 10 — Meteorological data obtained on-site during diving operations on August 21

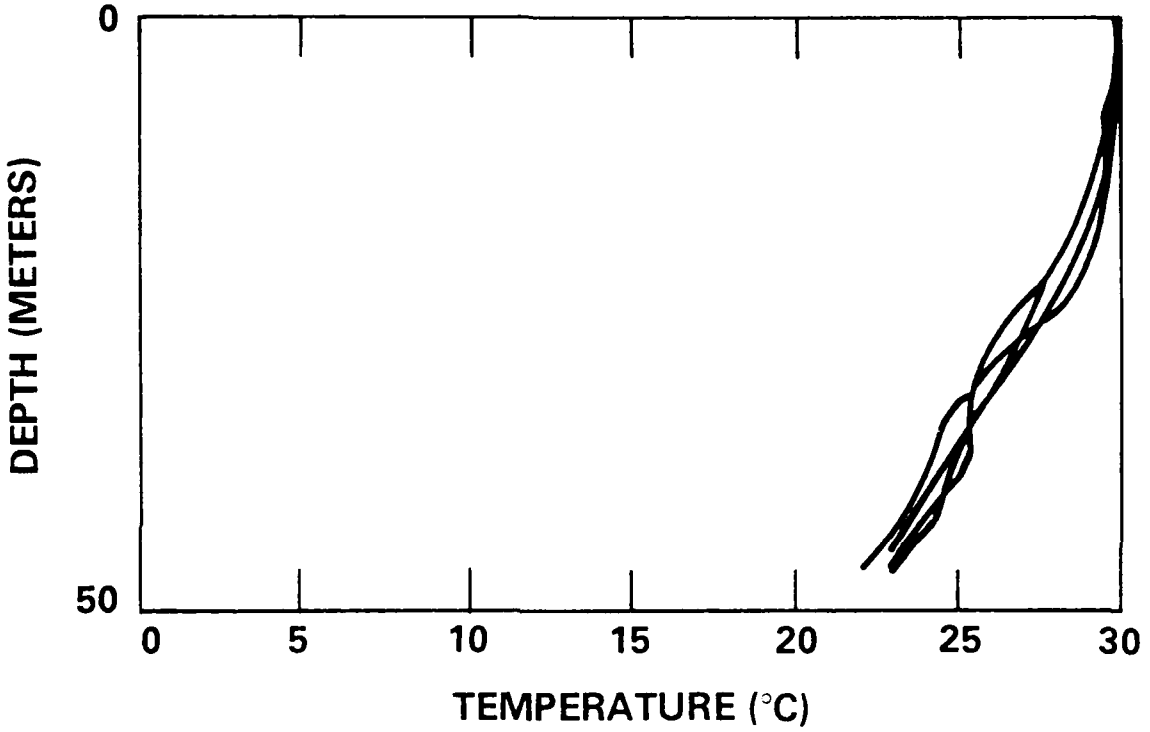

Fig. 11 — XBT data obtained on-site during operations on August 21

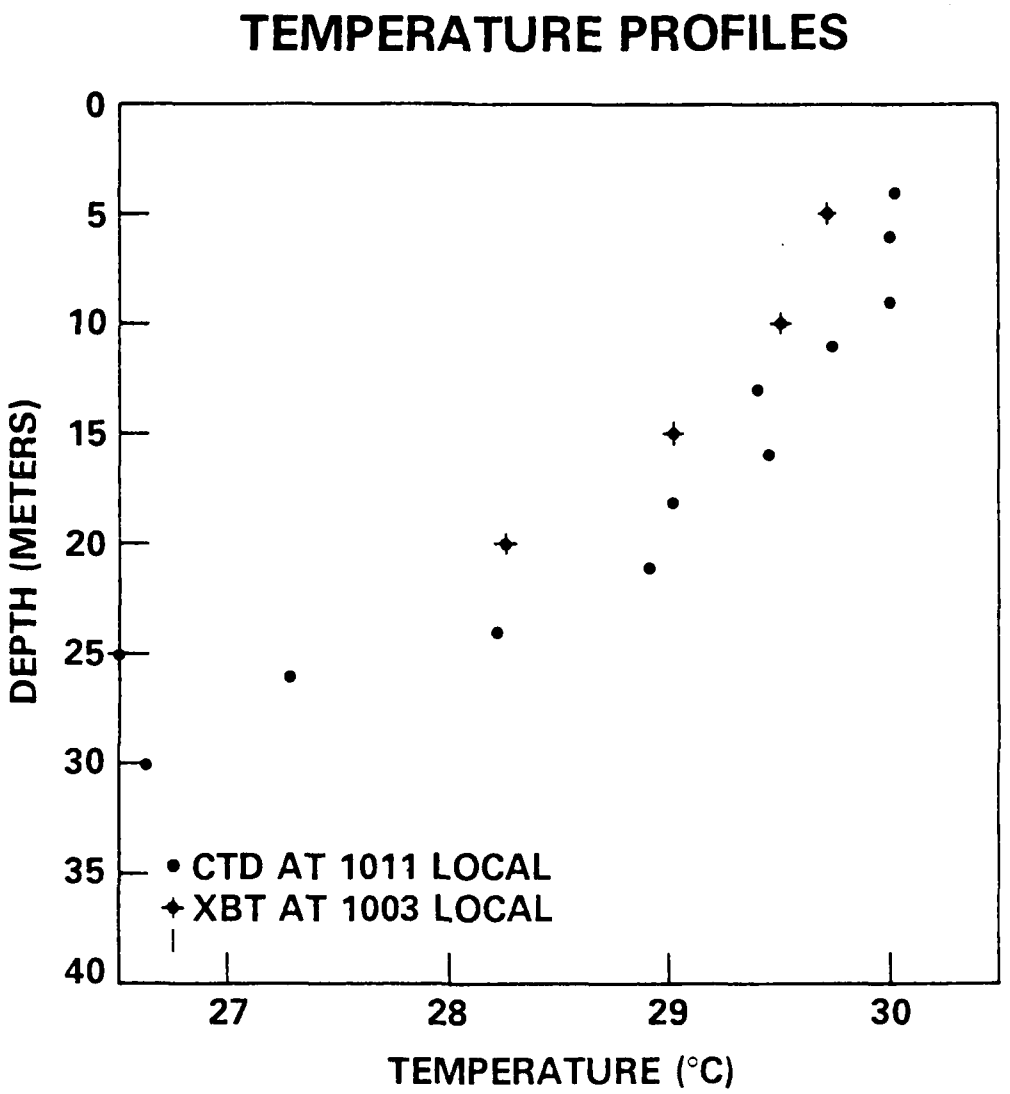

Fig. 12 — Comparison of XBT and CTD data

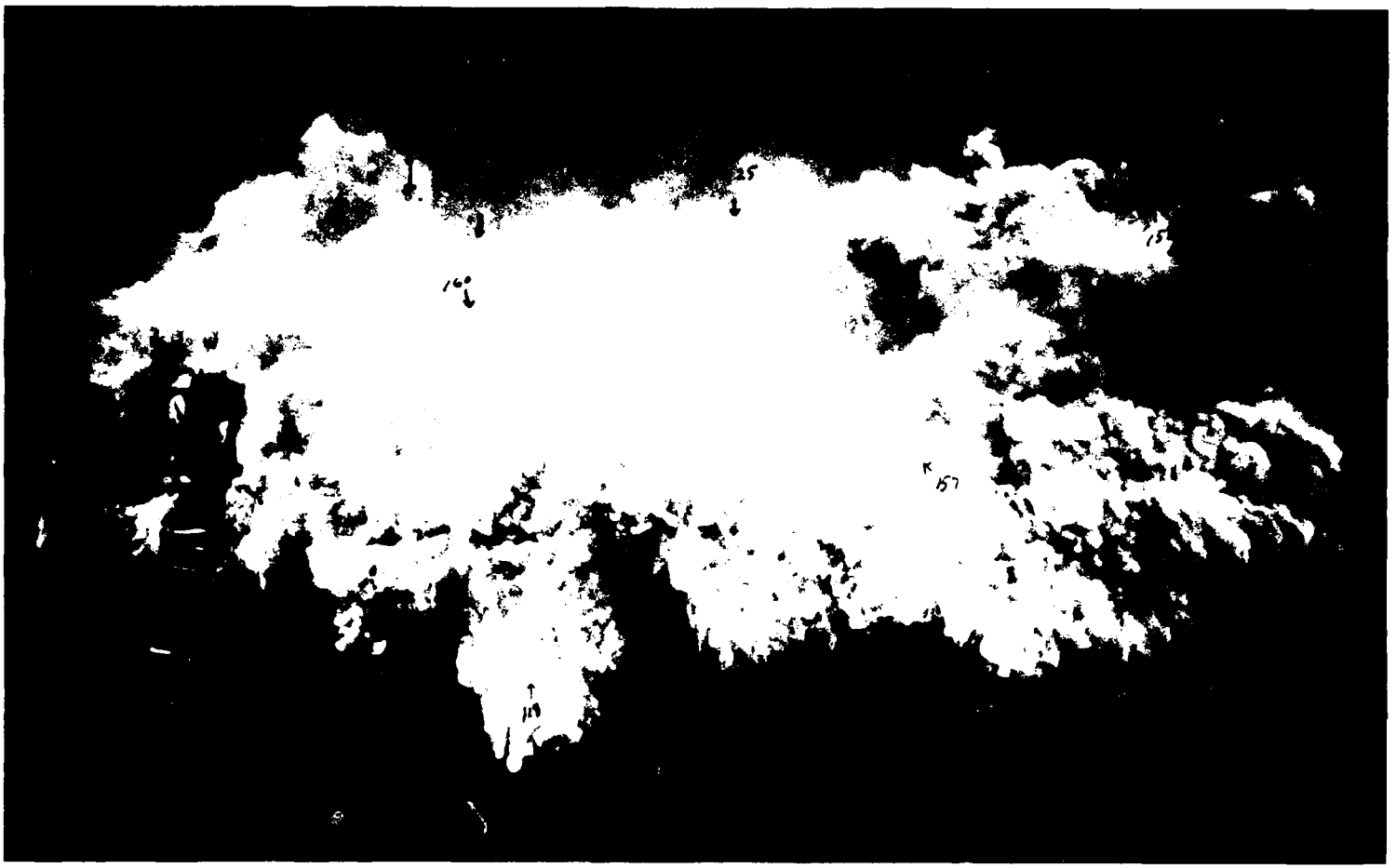

Fig. 13 — Dye sheet photograph

R-019

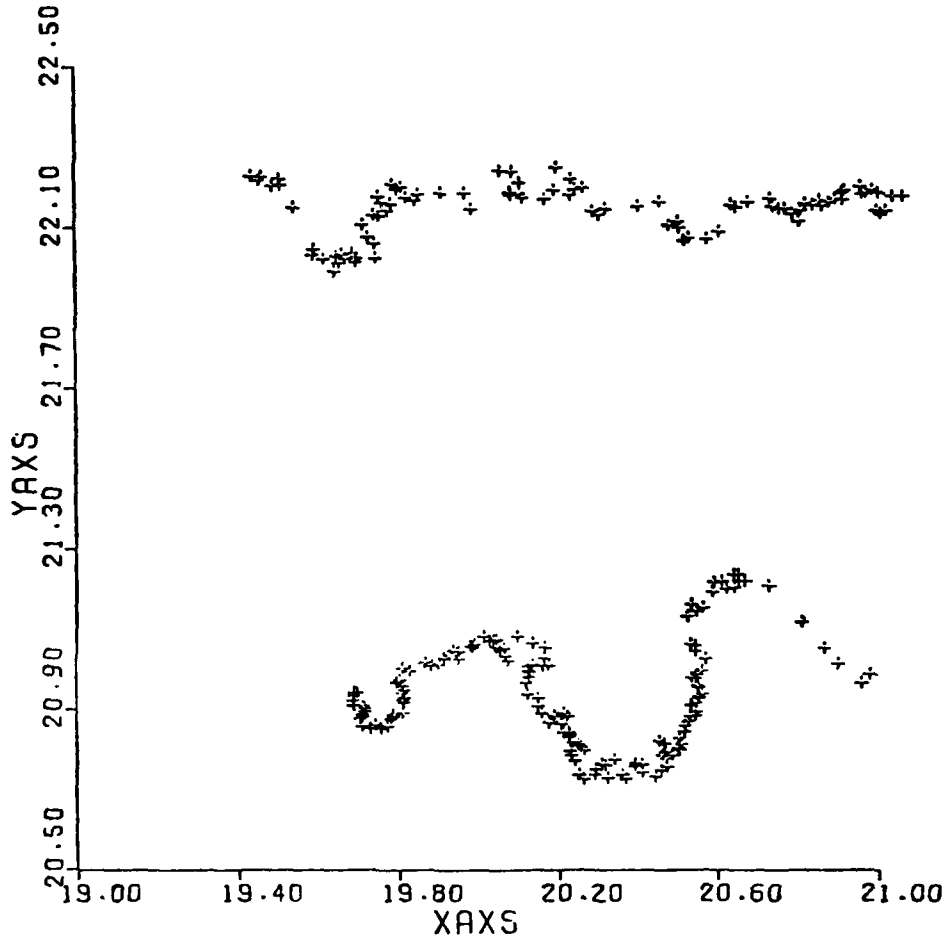

Fig. 14 — Top view pattern of the dye sheet determined from photogrammetric application to dye sheet photographs

NISC SUPPLEMENTARY REPORT

MENSURATION OF UNDERWATER PHOTOGRAPHY USING PHOTOGRAMMETRIC TECHNIQUES

Prepared for:

Naval Research Laboratory
Washington, D. C. 20375

Prepared by:

Naval Intelligence Support Center
Imagery Analysis Department
Imagery Exploitation Systems Division
Photogrammetry Systems Branch
Washington, D.C. 20390

Enclosure (1)

MENSURATION OF UNDERWATER PHOTOGRAPHY USING PHOTOGRAMMETRIC TECHNIQUES

TABLE OF CONTENTS

1. INTRODUCTION

This report describes a photogrammetric dimensional investigation of the dispersal pattern of a chemical dye discharged into the water off the coast of Florida by an investigative team from the Naval Research Laboratory (NRL). Photographs were taken by Navy divers at fixed time intervals using three underwater 35 millimeter cameras. The cameras were attached to a horizontal bar at fixed angles and distances apart to provide geometric qualities required for an analytical photogrammetric solution. This solution also required photographs exposed simultaneously from the three cameras at specified time intervals.

The objective of this study is to determine if the photogrammetric solutions used by the NISC Photogrammetry Systems Branch can provide the NRL team the dimensional components (vectors) of the dye pattern's ballooning characteristics caused by water variables acting upon it.

2. PROCEDURES

2.1 Materials Furnished

Three (3) rolls of 35mm color positives (approximately 100 frames) of the dye pattern were submitted for investigation and selection. The following information was provided to support the analytical solutions:

(a) Camera focal lengths (in water) -- 28.0mm
(b) Camera separation -- 1.0 meter
(c) Shutter release on camera -- Simultaneous
(d) Exposure interval (time lapse) -- Approx. 10 Sec
(e) Tilt of outer cameras axis toward center camera -- 20 degrees

2.2 Test Outline

Two dye dispersal tests were determined to be adequate for demonstrating the applicability of analytical photogrammetry to the NRL requirements. The time interval between photographs of the two tests was not to exceed 20 seconds because of the deformation of the dye pattern. Common image points from the photographs of the two tests were measured where possible for evaluation of the point vectors.

The data was reduced using the Analytical Photogrammetric Data Reduction Solution (APDARS) in order to determine the relative positioning of the cameras in object space as well as locating the object space coordinates of the points that were measured in image space.

Plots of the common image points were made from different view angles to show relative movement and ballooning effect at the different time intervals. Coordinate values and radial distances of an all point combination were also calculated for additional analysis.

2.3 Test BLOCKS

The APDARS solution calculates object space coordinates by tying or BLOCKING overlapping photographs together. Three photographs define a photogrammetric BLOCK. The photographs from the NRL problem were from different camera stations but covered the same area of the dye pattern. These photographs were synchronous and reflected the position of the dye pattern at that moment in time. The BLOCKS from the two NRL tests were subjected to the rigorous APDARS solution to determine the relative position and orientation of image space with respect to the object space. The fixed camera station distance (1.0 meter) was used to scale dimensions for true ground coordinate positions.

The following data defines each of the frames within the BLOCKS:

(a) BLOCK #1

	Frame	
CAM Position	Kodak	Block No.
Left	19A	20L or 201
Center	20A	20C or 202
Right	20A	20R or 203

(b) BLOCK #2

	Frame	
CAM Position	Kodak	Block No.
Left	21A	22L or 221
Center	22A	22C or 222
Right	22A	22R or 223

Block #1 contained 34 image points and BLOCK #2 32 image points. These points were selected for clarity of image, geometric position, and commonality between frames and BLOCKS.

2.4 Selection and Measurement of Points

The six photographs selected were enlarged 6X and printed on photographic paper as a base for marking and measuring the image points. These photographs are enclosed as Appendix A of this report.

Image points were selected and marked on the prints. The selection was made to provide strong geometry for an APDARS solution in each of the two BLOCKS. Also common points between the two BLOCKS were an important guideline in the point selection criteria. However, identification was difficult since the change of the image characteristics during the time interval made it nearly impossible to identify common points. Only five points were identified with any confidence as common between the two BLOCKS.

The movement of the camera stations relative to the dye pattern (approximately 1.0 meters) affected point identification because of different view angles at close range.

Measurements of each image point on the photographs were made on an ALTEC digitizer to an accuracy of 0.1 millimeters.

2.5 BLOCK Solution

Preprocessing and organization of the data for input into the APDARS solution requires care and experience. The APDARS solution is a lengthy procedure which is discussed briefly in Appendix B of this report. This discussion defines the basic concept of processing the data and the general solution without analyzing the math model.

Appendix C contains the computer listings of the iterative solutions of both BLOCK adjustments, the final products of camera station positions, attitudes, point positions and the image coordinate values measured on the ALTEC digitizer.

3. EVALUATION

Based on residuals of the X, Y, Z rectangular coordinates in the APDARS solution of both BLOCKS, the positional accuracy of each image point is estimated to be within 10 millimeters. The object space values in meters for each of the BLOCKS are listed as figures 1 and 2.

As noted before, only five of the image points are common to both BLOCKS. The direction and magnitude of movement of these points during the time interval between the two BLOCKS were main factors to be determined by this evaluation. However, the lack of a fixed reference plane common to both BLOCKS prevented a vector determination for any of the points. In figures 3 and 4, radial distances are given between common points which show differences caused by movement of points in both time frames.

Represented in the radial distances is the ballooning effect of the dye pattern caused by the variable forces acting in the water. Although it is not possible to compute vectors of movement caused by these variables, changes can be shown between common points by computing radial differences at different time intervals.

The following lists are radial differences of the five common points:

Pt. IDS		BLOCK #1	BLOCK #2	(2 - 1)
		(Meters)		
From	To			
09	10	.089	.082	-0.007
09	13	.603	.619	0.016
09	16	.766	.699	-0.067
09	27	1.373	1.446	0.073
10	13	.543	.573	0.030
10	16	.713	.656	-0.057
10	27	1.424	1.501	0.077

BLOCK #1

ID.	X	Y	Z
0005	19.153	20.896	17.730
0006	19.251	20.989	17.726
0007	19.407	21.021	17.764
0008	19.436	21.189	17.810
0009	19.702	20.926	17.781
0010	19.741	20.859	17.736
0011	20.071	20.991	17.808
0012	20.179	20.862	17.751
0013	20.269	20.734	17.706
0014	20.333	20.740	17.703
0015	20.375	20.731	17.725
0016	20.441	20.725	17.759
0017	20.465	20.741	17.766
0018	20.335	21.003	17.819
0019	20.702	21.131	17.892
0020	20.670	21.040	17.755
0021	20.972	20.961	17.793
0022	20.948	21.035	17.811
0023	21.086	22.160	17.772
0024	20.837	22.156	17.735
0025	20.520	22.141	17.717
0026	20.416	21.629	17.909
0027	20.197	22.207	17.791
0028	19.965	22.187	17.742
0029	19.668	22.094	17.670
0030	19.427	22.209	17.758
0031	19.006	22.431	17.794
0032	19.010	22.112	17.755
0033	18.658	22.398	17.793
0034	18.524	22.259	17.766

Fig. 1 — Final X, Y, Z point coordinates (meters) — BLOCK #1

BLOCK =2

ID.	X	Y	Z
0009	18.704	20.777	17.664
0010	18.723	20.713	17.636
0013	19.264	20.536	17.574
0016	19.345	20.506	17.615
0027	19.196	22.137	17.658
0111	18.911	20.841	17.578
0117	19.369	20.541	17.576
0118	19.334	20.734	17.644
0120	19.762	20.832	17.603
0121	19.824	20.792	17.557
0123	20.074	22.169	17.638
0124	19.863	22.133	17.612
0125	19.541	22.079	17.572
0128	19.074	22.156	17.667
0129	18.688	22.023	17.641
0130	18.468	22.095	17.767
0149	20.259	22.247	17.664
0150	20.913	22.196	17.652
0151	20.698	22.212	17.649
0152	20.556	22.148	17.624
0153	20.643	22.060	17.582
0154	21.109	20.871	17.426
0155	20.599	20.902	17.532
0156	20.358	20.908	17.556
0157	20.227	21.286	17.696
0158	20.045	20.866	17.550
0159	19.694	20.841	17.539
0160	18.920	21.656	17.790

Fig. 2 — Final X, Y, Z point coordinates (meters) — BLOCK =2

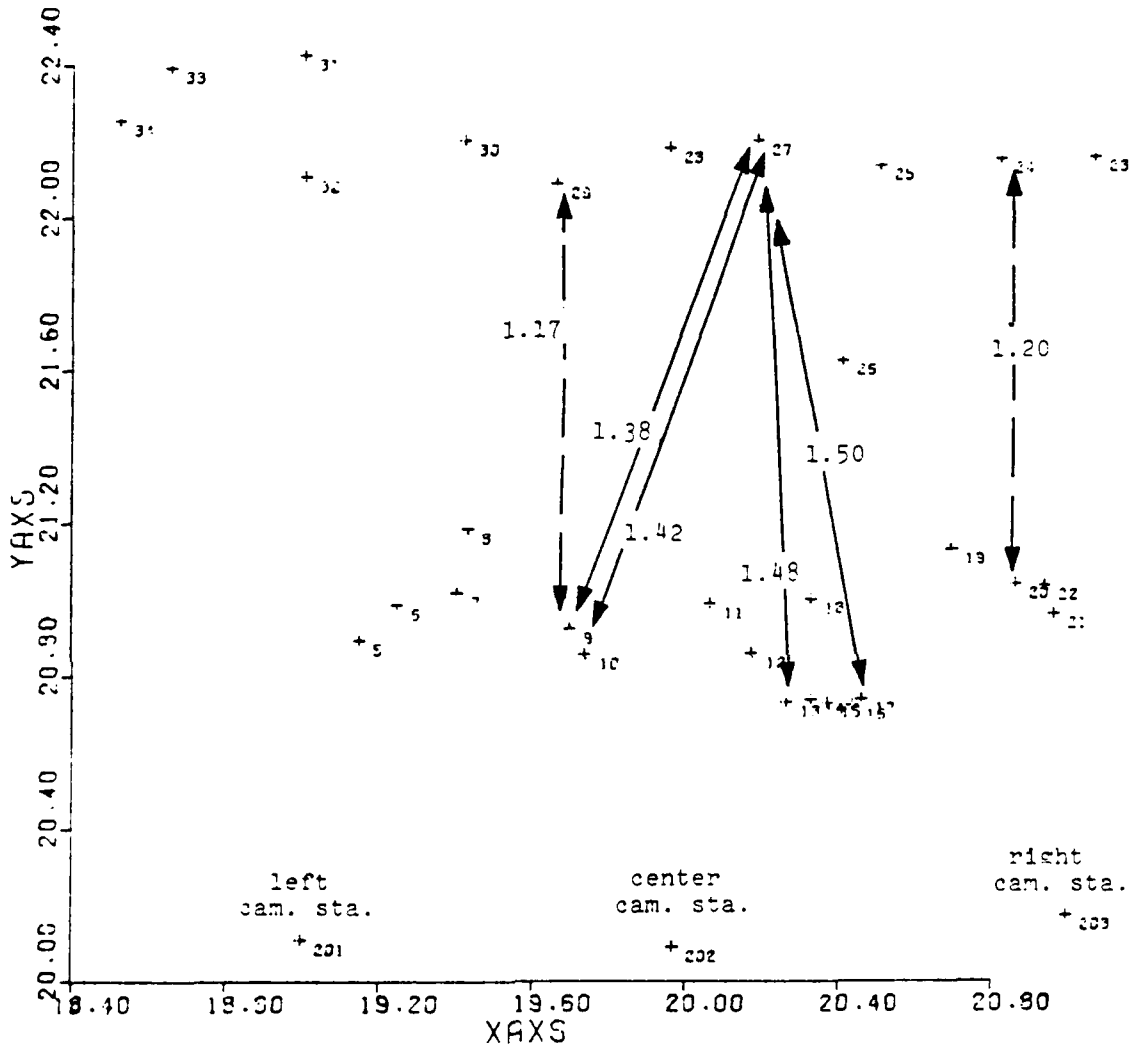

Fig. 3 — Radial distances of points — BLOCK #1

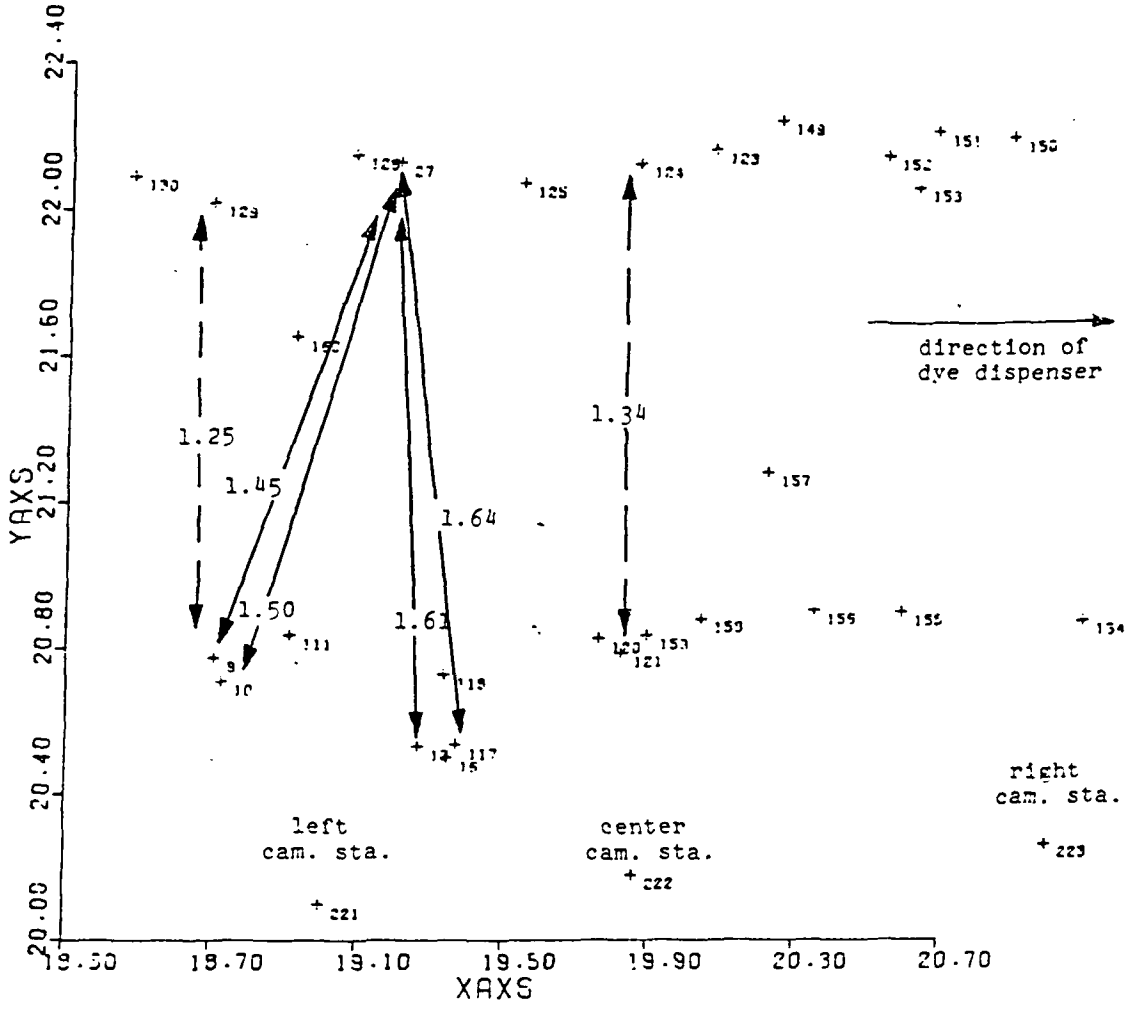

Fig. 4 — Radial distance of points — BLOCK #2

Pt. IDS		BLOCK #1	BLOCK #2	(2 - 1)
		(Meters)		
From	To			
13	16	.180	.096	-0.084
13	27	1.477	1.605	0.128
16	27	1.502	1.638	0.136

The distance of travel between BLOCK #1 and BLOCK #2 was computed to be approximately 1 meter. This movement is attributed to either the drift of the dye or the camera station movement or a combination of both. The same camera station values with slight deviations in the parameters were used in the two independent solutions. These values are as follows:

BLOCK #/Sta No.	X (m)	Y (m)	Z (m)	Omega °	PHI °	Kappa °
1-201	19.0	20.11	19.32	29.26999	-22.3100	-0.39000
2-221	19.0	20.10	19.91	30.05899	-21.39200	0.09770
Difference	0.0	0.01	0.02	-0.78900	0.91800	0.29230
1-202	19.97	20.09	20.20	26.70982	0.21015	0.01731
2-222	19.86	20.18	20.21	25.56479	-1.12191	0.31984
Difference	0.11	-0.09	0.01	1.14503	1.33206	-0.30253
1-203	21.0	20.17	1983	30.25954	28.75157	-0.88124
1-223	21.0	20.26	19.90	28.29124	29.11395	-0.10079
Difference	0.0	-0.09	-0.07	1.96830	-0.36238	0.78045

The small deviations of the camera station position will cause some differences but not of the 1 meter magnitude as shown by the differences in position of the following common points of the two sets:

SET # - PT. No.	X (m)	Y (m)	Z (m)
1 - 9	19.70	20.93	17.77
2 - 9	18.70	20.78	17.68
Difference	1.0	0.15	0.10
1 - 10	19.74	20.86	17.74
2 - 10	18.72	20.71	17.64
Difference	1.02	0.15	0.10
1 - 16	20.44	20.72	17.76
2 - 16	19.34	20.51	17.62
Difference	1.10	0.21	0.14
1 - 27	20.20	22.21	17.79
2 - 27	19.20	22.14	17.66
Difference	1.0	0.07	0.13

The look-angle of the cameras defined the orientation of the coordinate system that was established for the BLOCKS. This angle was estimated from the plumbob that was imaged in the photograph. This estimate is probably in error up to 10°.

Figures 5, 6, 7, 8, 9, and 10 represent the side, top, and front views of the dye pattern test areas which are based on the above estimated orientation.

The cameras are positioned above the test area and are pointed down at a 35° to 45° angle. Their locations are shown in figures 11 and 12 which give meter distances of the center camera from both edges and center of the photographs. These views recorded only the image of the top side of the dye pattern. A different position of the cameras would be required if the bottom side of the dye pattern is to be studied.

3.1 Single Photo Solution

A single photo solution was used to outline the position of the edges of the dye pattern on frames #202 and #222. This type of solution required the position and orientation of the camera stations that were computed by the APDARS solution. In addition to this data, one of the coordinates (X, Y, or Z) of the image point being measured is required in order to compute the other 2 remaining coordinates. The supplied coordinate for the solution is a critical element in the final accuracy of the point being measured, especially in oblique photography.

Figure 13 shows an outline of the rectified coordinates of the dye pattern edge on frame #202. The Z value was selected as the given coordinate and assigned a numerical value of 17.75 meters for all the points. This is near the mean of the Z values which was determined in the APDARS solution. The spread was from 17.67 to 17.91 meters. Frame #222 was also measured using the same technique. The Z value was also the common coordinate in this solution with a value of 17.60 meters. The spread was 17.42 to 17.79 meters. By overlaying the plots of these two frames, the change and/or movement can be noted in this 20 second time period. (Large plot sheets, Appendix D, are enclosed for this purpose.) Movement of up to 0.07 meters is noted on both edges of the dye pattern. This is accurate to within 0.02 meters.

To check the critical effect of an error in the Z value for each point, the Z value was changed from 17.60 to 17.65 meters (difference of 0.05) on frame 222 and the solution reran. Points were found to shift at variable magnitudes from 0.01 to 0.07 meters with the larger shift being in the upper portion of the frame in the direction of the photographic tilt angle. Vertical photographs of the dye pattern could eliminate a large percentage of the error that is caused by error in the Z value.

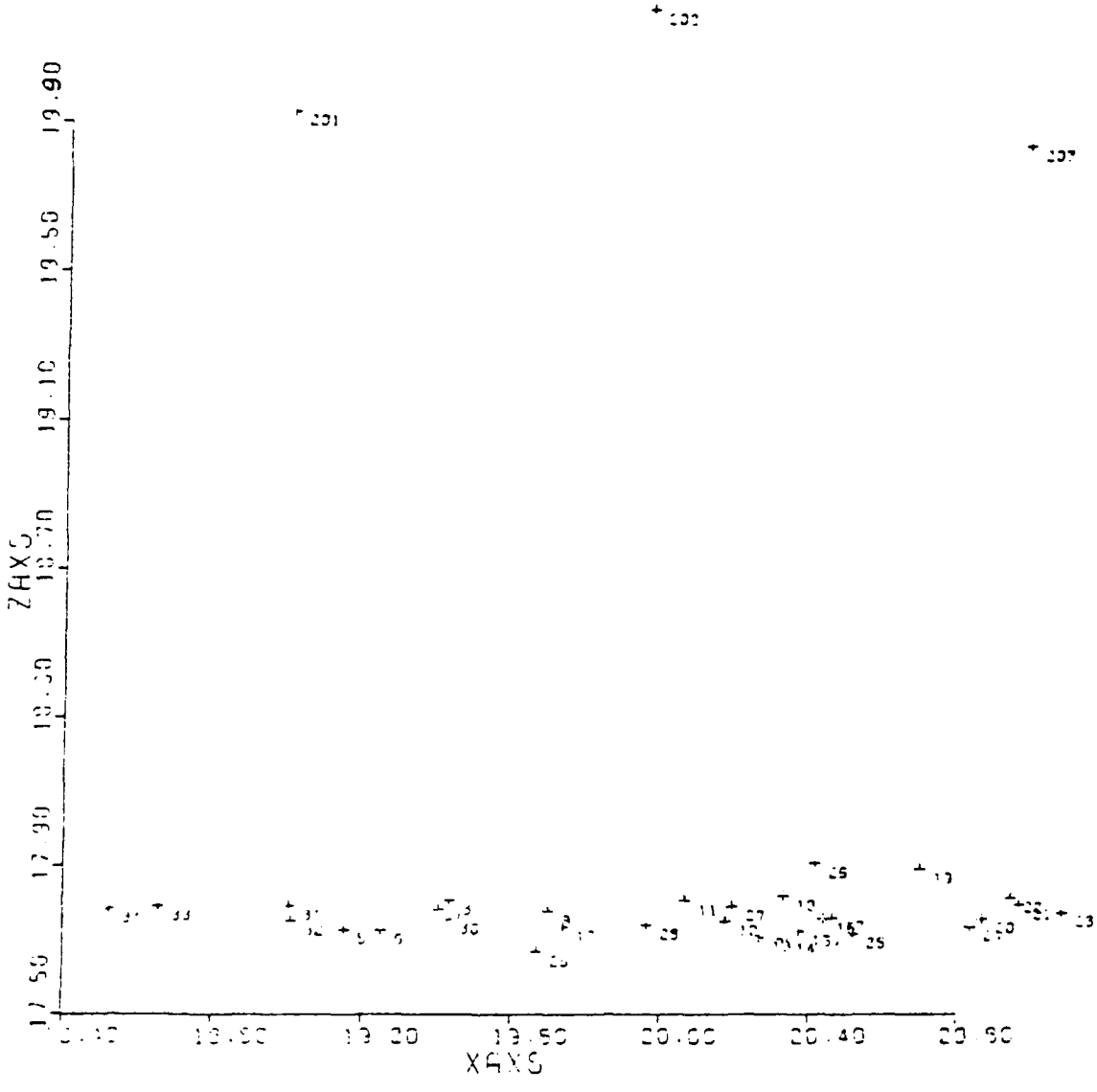

Fig. 5 — Side view (XZ plane in meters) — BLOCK #1

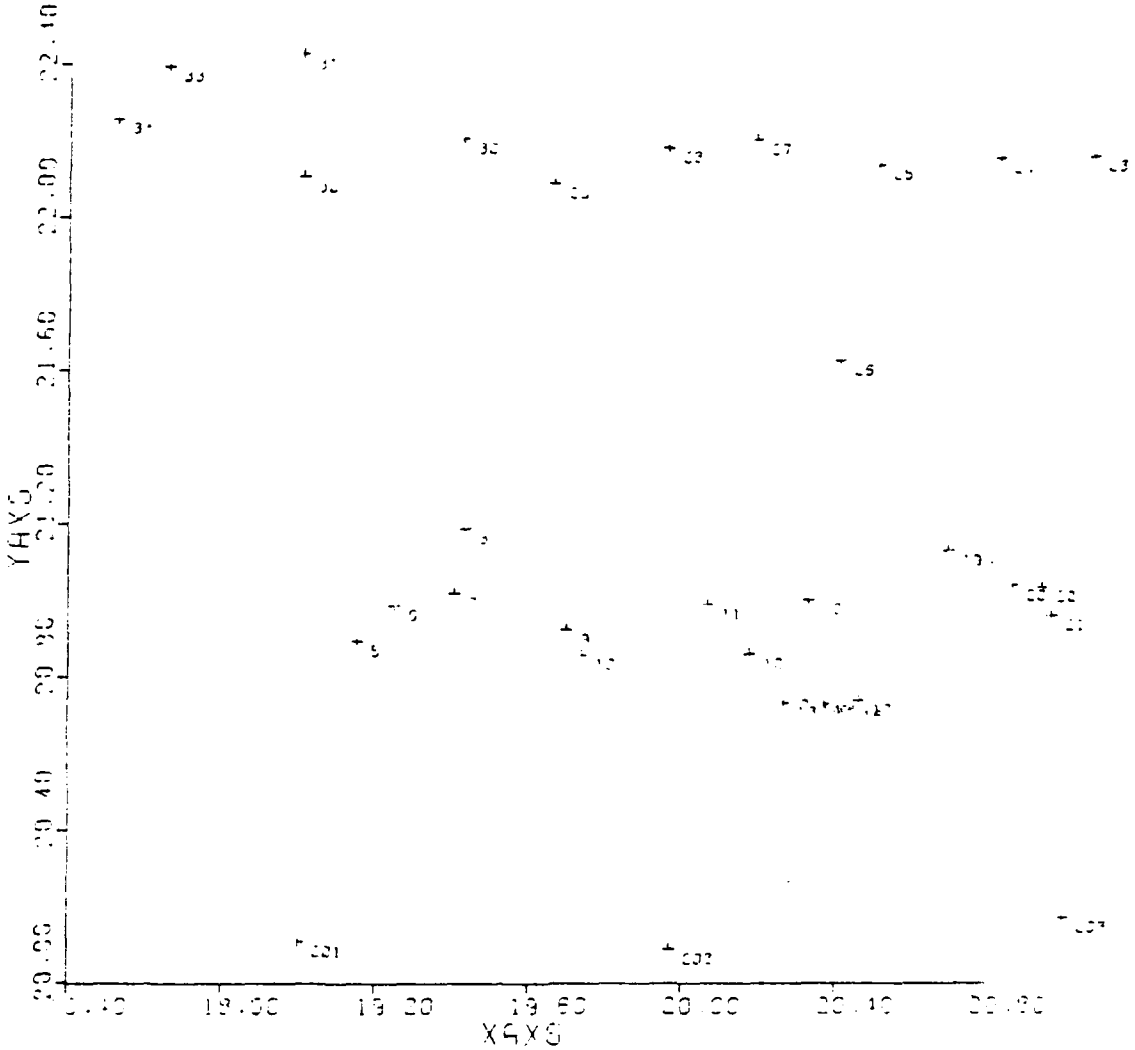

Fig. 6 — BLOCK #1 — top view (XY plane in meters)

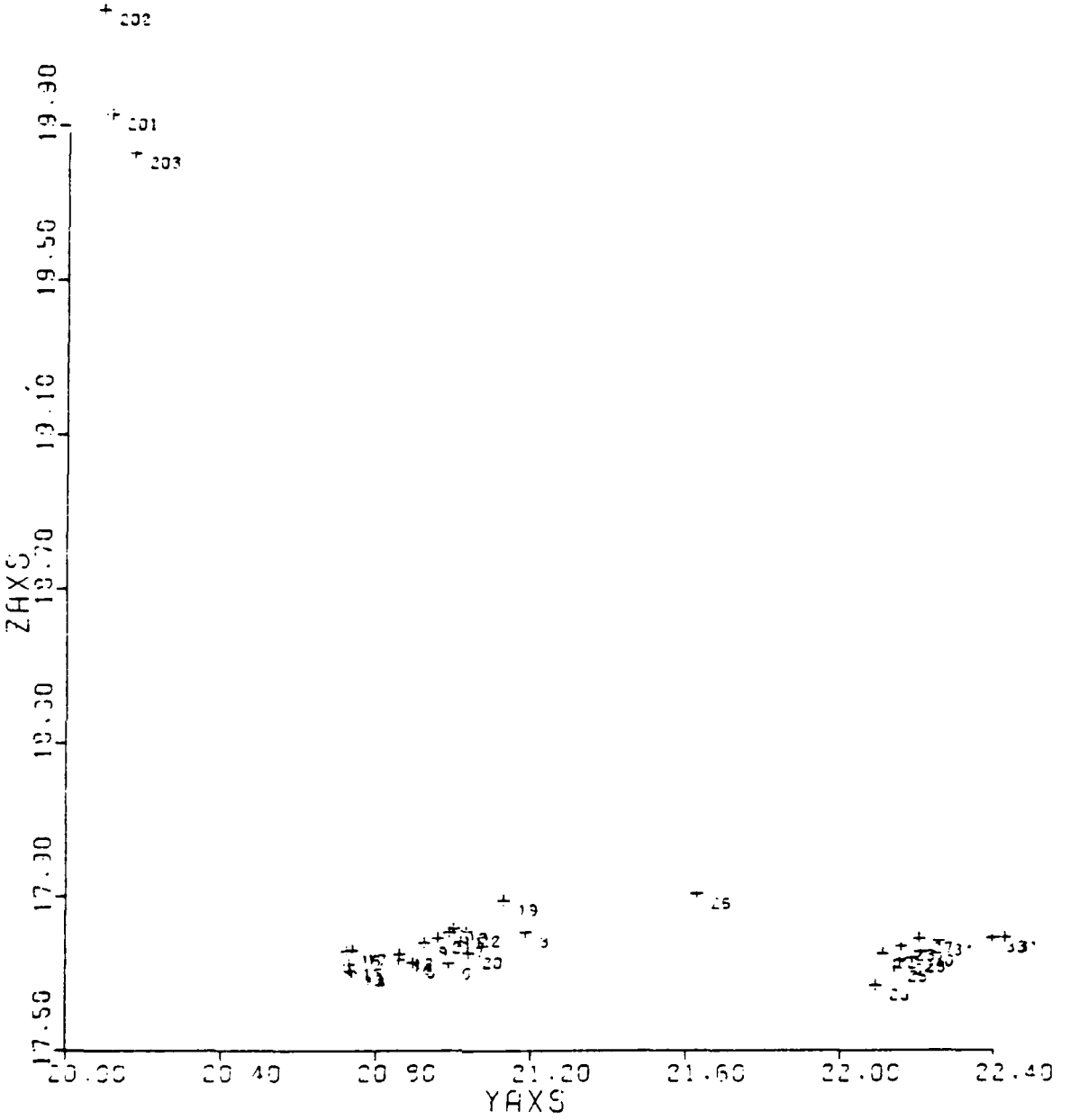

Fig. 7 — BLOCK =1 — front view (XZ plane in meters)

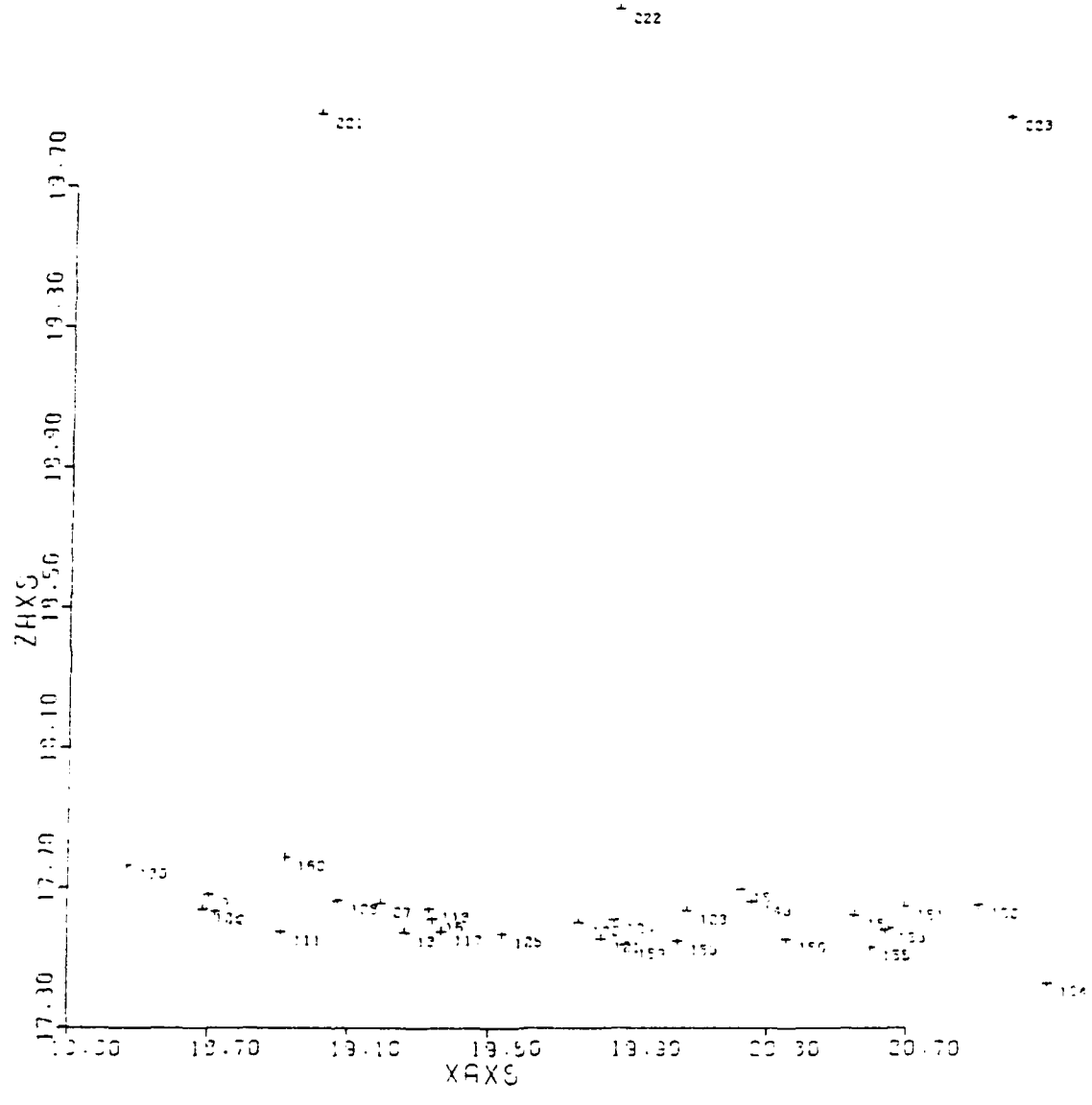

Fig. 8 — BLOCK #2 — side view (XZ plane in meters)

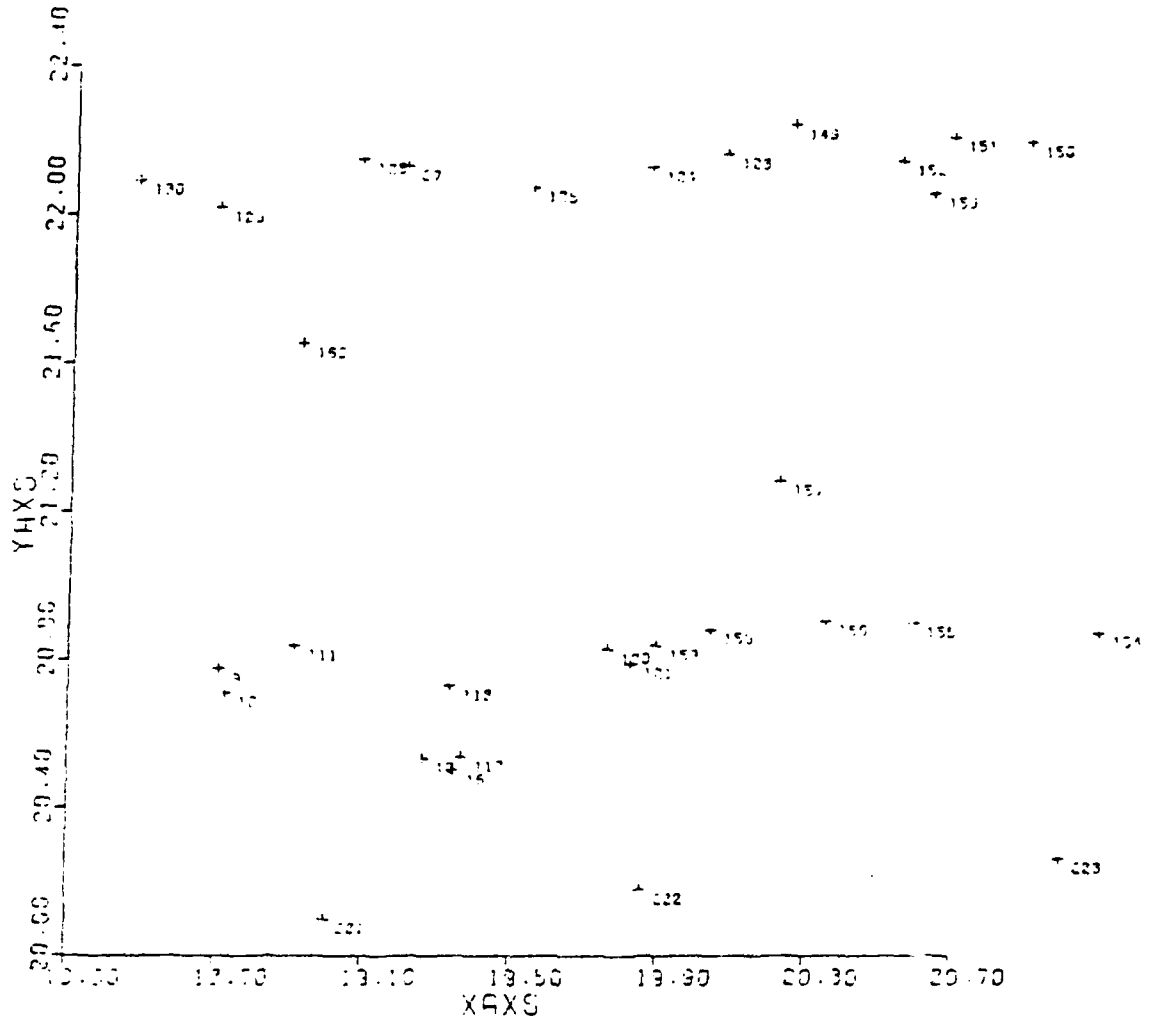

Fig. 9 — Top view (XY plane in meters) — BLOCK #2

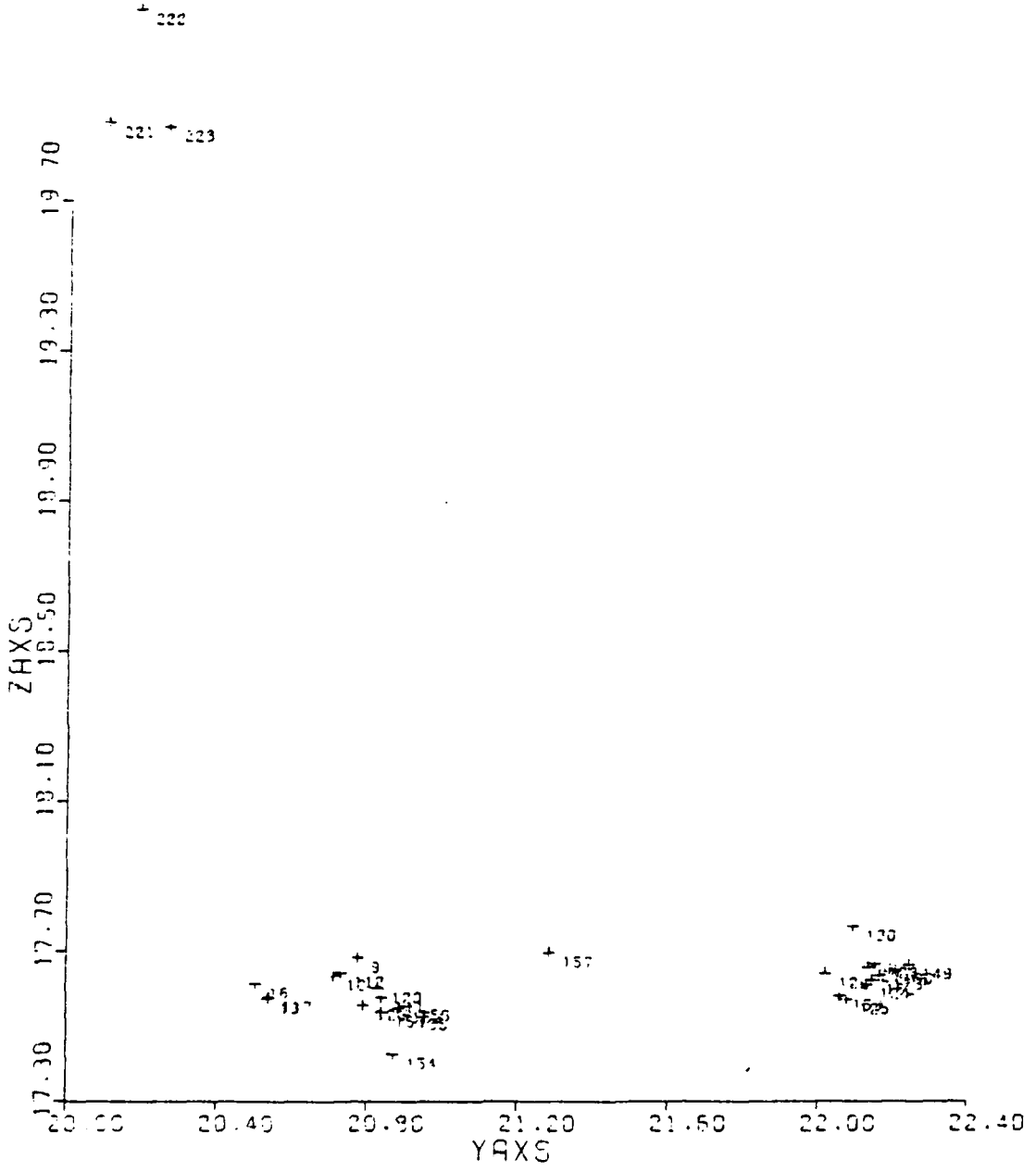

Fig. 10 — BLOCK #2 — front view (XZ plane in meters)

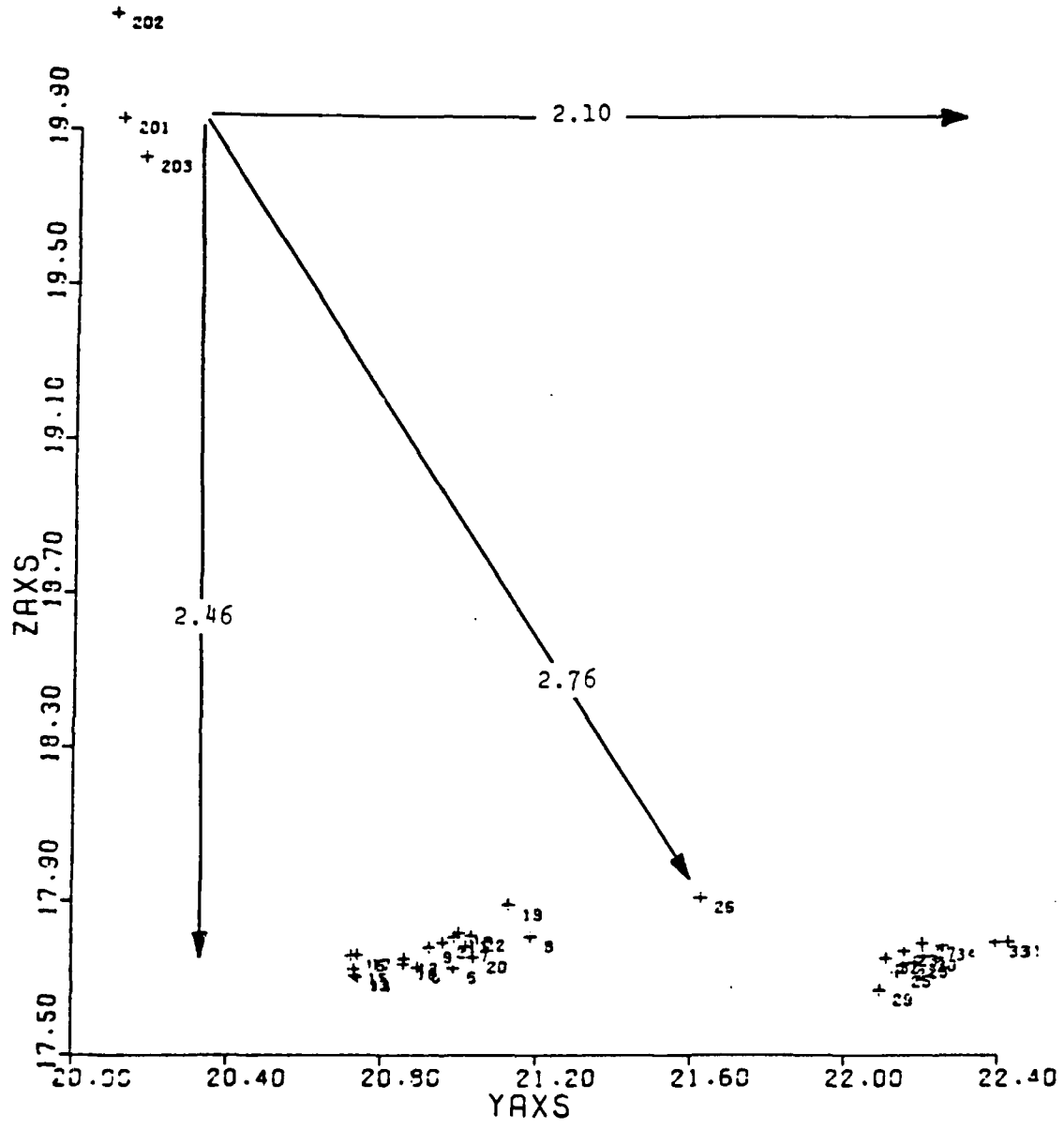

Fig. 11 — Camera stations location — BLOCK #1

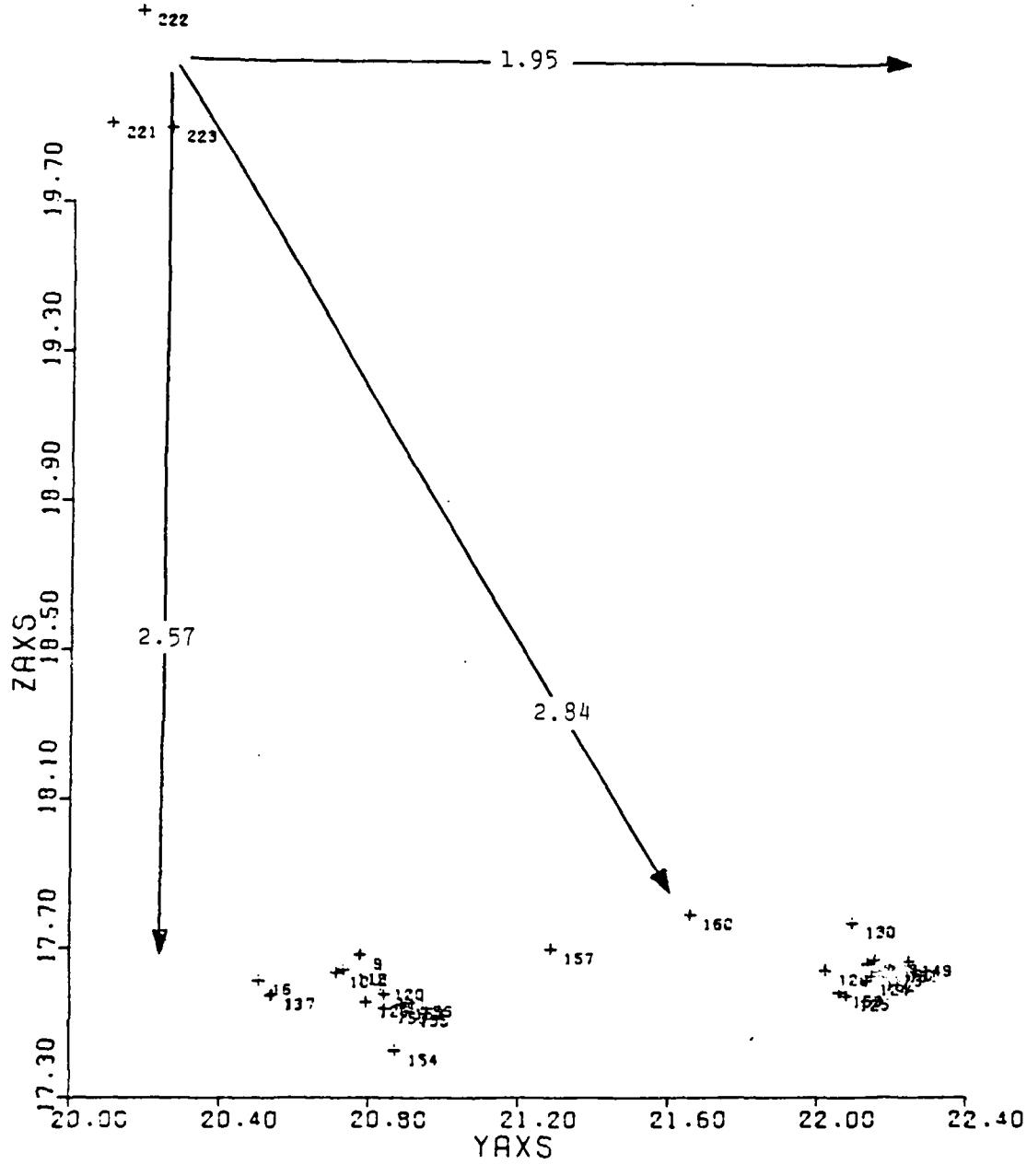

Fig. 12 — Camera station location — BLOCK =2

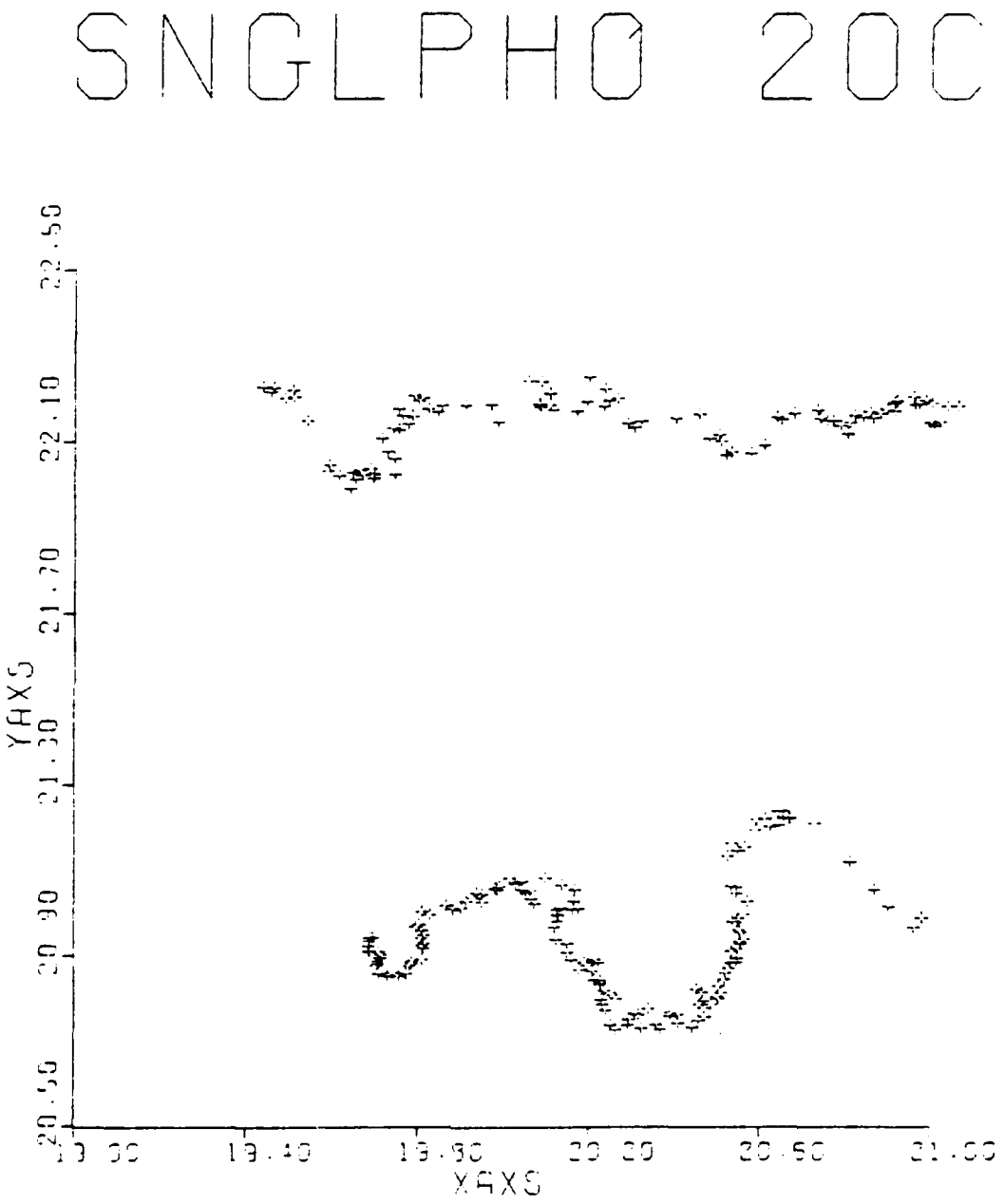

Fig. 13 — Rectified plot of dye pattern edge — BLOCK =1

4. CONCLUSIONS

There were only minor problems in establishing an APDARS solution for the selected underwater photographs. The positional errors of the solution were considered to be within 10 millimeters of the points' true positions. This is based on the reliability of the distances between the camera stations (scale factor) furnished by NRL. The accuracy of the end product cannot be any better than this scale factor.

Movement of points relative to a different time-span exposure can be traced within the accuracy as stated above. The major problem encountered in these tests was identification of common points. Changes in the shape of the image would be reduced and more identifiable if the time span were shortened between photographs. However, the interval of exposure must be of sufficient duration to reflect dye pattern movement which is the objective of the study.

The drift of the cameras relative to the scene of the first BLOCK hampered common point identification. Image points were obscured by large dye plumes as the cameras drifted. The film was exposed at very close range and any small movement of the cameras caused an exaggerated movement of the image in the focal plane which is representative of the camera separation with respect to object distances (base-height ratio).

The single photo solution has a variable factor of accuracy which was caused by the estimate of one of the X, Y, Z components. In these tests, the Z component was estimated in the solution. To improve the accuracy, measurements should be made on a stereo comparator or a concentration of common image points should be selected for the APDARS solution in the area where the single photo solution is to be performed.

The performance of the ADPARS solutions in this test is considered a success. The accuracy of such solutions can further be improved by continued evaluation of the application of analytical photogrammetric techniques and implementation of the recommendations.

5. RECOMMENDATIONS

- A fixed place of reference is necessary in the area to be tested to determine direction and magnitude of movement of measurable image points in the dye pattern.
- The accuracy of such solutions can be improved by camera calibration and by placing a scale within the photographed area.
- Time intervals between BLOCK areas should be less than 20 seconds to aid in image point identification.
- Cameras should remain in the same position relative to the scene being recorded.
- Cameras should also be moved closer together instead of the one meter separation. This should be evaluated using the Base-Height Ratio principle.

FLOW DIAGRAM -BLOCK ADJUSTMENT

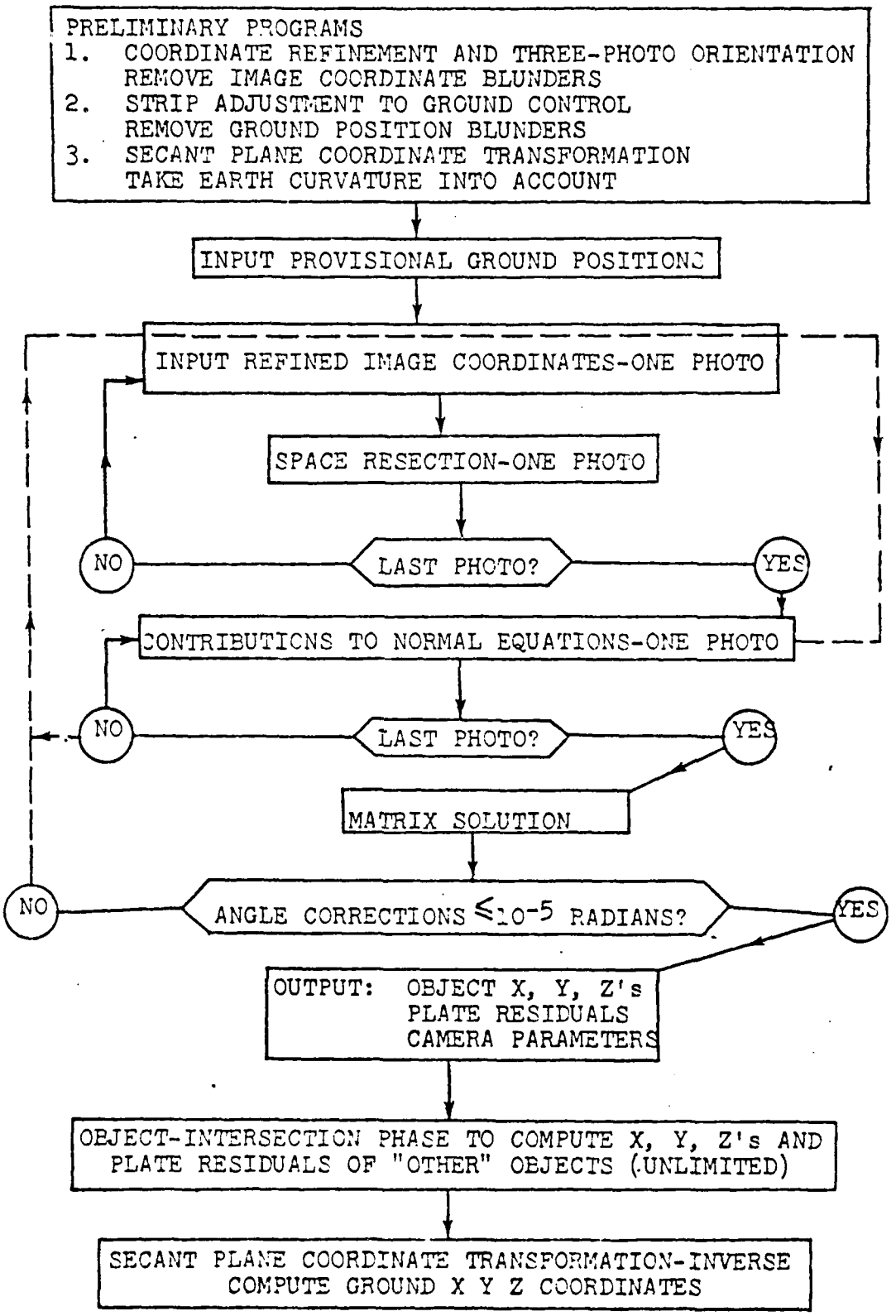

APPENDIX A

Appendix A contains the six (6) photographic prints used for selection and marking of image points used in the two (2) photogrammetric BLOCKS. These prints were also used for mensuration of the image points on the ALTEC digitizer.

R-018

R-017

R-016

R-015

R-014

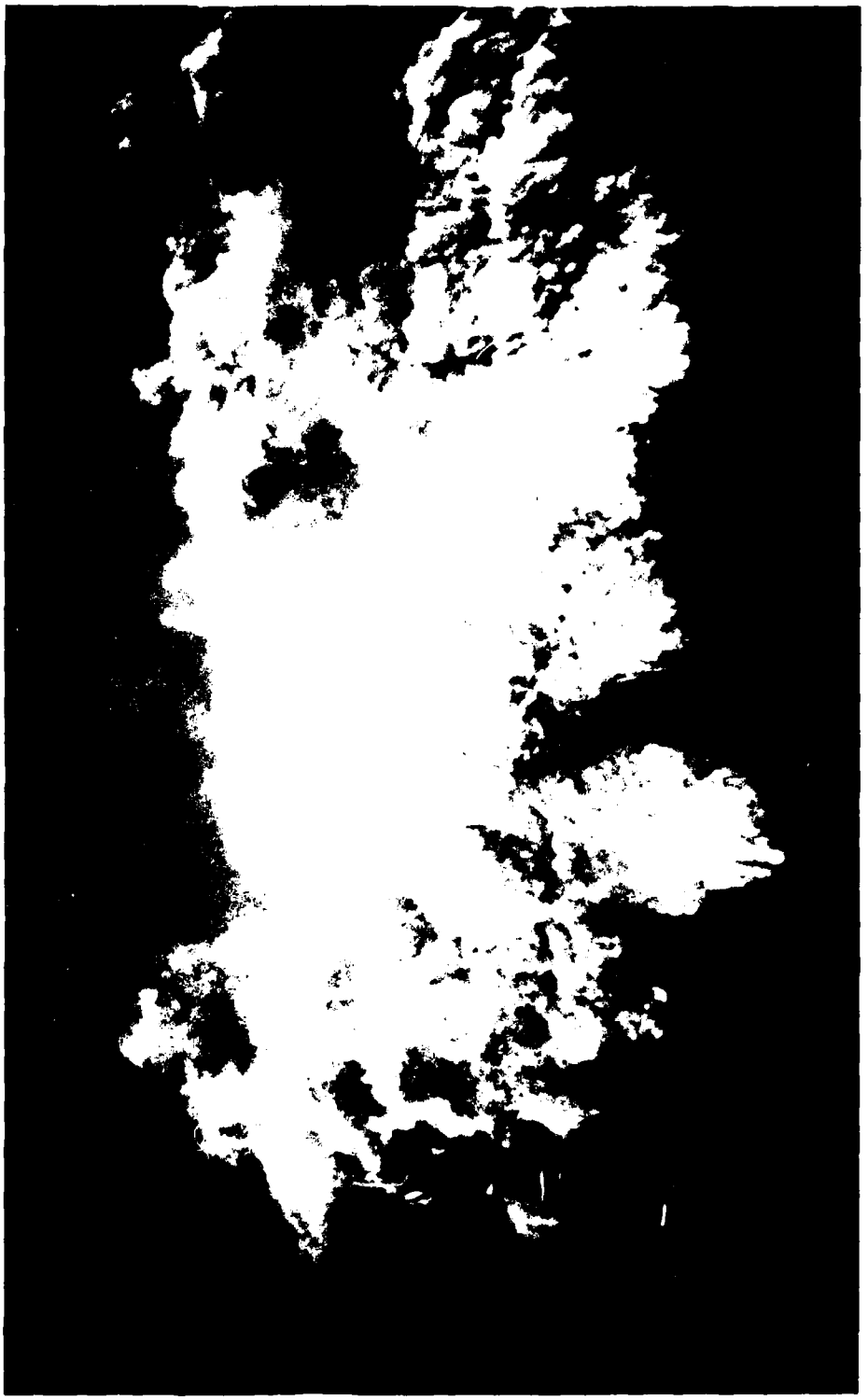

R-020

APPENDIX B

This appendix provides a general outline of a multi-photo BLOCK adjustment solution written by the Coast and Geodetic Survey. The basic math model of the APDARS solution utilizes the same principle photogrammetric equations. APDARS varies primarily in the data processing procedures and matrix configuration in the computer programs. The APDARS solution was designed for NISC to reduce data from close range frame photography and is operator oriented for error analysis and editing capabilities.

BLOCK ADJUSTMENT

Block adjustment is the simultaneous solution of the absolute orientation (three angular elements of orientation w ϕ k and three linear elements of position Xo Yo Zo) of all the photographs in the block together with a determination of the finalized ground coordinates for each object. The collineation principle is imposed on these unknowns in a single large simultaneous solution that minimizes the observational discrepancies according to least squares. The major task of the block adjustment program is the solution of the large number of simultaneous equations in a least squares manner that efficiently utilizes the memory capacity of the computer. After the block adjustment is completed, the adjusted secant plane coordinates are transformed back into the original ground coordinate system by applying the secant plane transformation program in its inverse mode.

The original collinearity equations (17) and (18) cannot be used to solve this problem because the camera parameters do not appear as linear and independent unknowns as is required for a least squares solution. Such a least square solution is necessary because the photographs and images provide more equations than there are unknowns. It is therefore necessary to use the linearized collinearity observation equations obtained by applying the Taylor's Expansion Series to the original collinearity equations. Since the second and higher degree terms of the Series have been neglected, it will be necessary to iterate the least square solution.

INITIAL PARAMETERS FOR THE BLOCK ADJUSTMENT SOLUTION

In order to use the linearized observation equations provided by Newton's Method we must have initial approximations for the unknown parameters which are reasonably close to the correct values. The initial approximations of the x and y image coordinates are provided by the refined image coordinates obtained by processing the observed image coordinates through the coordinate refinement phase of the three-photo orientation program. The subsequent strip adjustment and secant plane transformation programs provide the initial approximations of the X Y Z coordinates for the pass-point objects and the control stations. What is lacking at this point are good initial approximations of the w ϕ k Xo Yo Zo camera parameters for each plate in the block. Note that the finalized camera parameters developed by the three-photo relative orientation computations cannot be used because the three-photo computations are completely independent from any ground control. The three-photo solution simply computes the relative orientation of all the photographs in the strip relative to one another in an arbitrary system in which the first plate in the strip is considered to be untilted and its camera lens is the origin of the coordinate system for the strip, i.e. w ϕ k Xo Yo Zo of the first plate in the strip is set equal to zero.

The initial values for the w ϕ k Xo Yo Zo camera parameters of each photograph in the block can be obtained by performing a resection solution on each picture. See previous discussion on RESECTION. The linearized collinearity equations used are:

$$\boxed{v_x = (P_{11}+P_{12}dw+P_{13}d\phi+P_{14}dk-P_{15}dXo-P_{16}dYo-P_{17}dZo)/A_3B}$$

$$\boxed{v_y = (P_{21}+P_{22}dw+P_{23}d\phi+P_{24}dk-P_{25}dXo-P_{26}dYo-P_{27}dZo)/A_3B}$$

The dX dY dZ terms are not present because the X Y Z coordinates now available for the pass-point objects are held constant during the least squares resection solution. A minimum of 3 pass-point objects and their images are required to achieve this solution. In practice, between 5 and 9 pass-points are used to resect each photograph.

The space-resection computation then fits the image data from each photograph to the corresponding provisional X Y Z coordinates and thereby determines initial values for the camera parameters. The iterative computation is terminated when the computed corrections dw dϕ dk to the angular camera parameters are each less

0.00001 radians (two arc-seconds). No more than 3 iterations are usually needed in practice to reach this condition because the solution converges rapidly.

The resection phase of the block adjustment program is applied and solved for each photograph in turn only <u>once</u>; if a second iteration of the block adjustment camera orientation phase is required, the resection phase is circumvented.

THE BLOCK ADJUSTMENT CAMERA ORIENTATION PHASE

After resecting each photograph, the program proceeds to the least squares block orientation phase for the simultaneous solution of the absolute orientation of all the photographs in the block and the computation of the final X Y Z coordinates for each object. These objects consist of the pass-point objects and the control stations.

For each image created by these objects on every photograph in the block, we write the two linearized collinearity observation equations. All the terms are present in the equations thereby permitting the w ϕ k Xo Yo Zo of each camera and the X Y Z of each object to change during the solution as needed to minimize the observational discrepancies v_x and v_y. The observation equations thus are:

$$\begin{bmatrix} v_x = (P_{11} + P_{12}dw + P_{13}d\phi + P_{14}dk - P_{15}dXo - P_{16}dYo - P_{17}dZo + P_{15}dX + P_{16}dY + P_{17}dZ)/A_3B \\ v_y = (P_{21} + P_{22}dw + P_{23}d\phi + P_{24}dk - P_{25}dXo - P_{26}dYo - P_{27}dZo + P_{25}dX + P_{26}dY + P_{27}dZ)/A_3B \end{bmatrix}$$

All of the P-terms can be computed using the initial approximations of w ϕ k Xo Yo Zo for each camera and the initial values of X Y Z for each object together with the x and y refined image coordinates.

WEIGHTING THE SOLUTION FOR IMAGE QUALITY

It is logical to want to weight the least square solution in favor of those observation equations provided by the better quality images because their equations are more reliable. Image quality is a function of many variables of which the most important are lens resolution and the type of ground object creating the image. Those images near the center of a photograph are resolved with greater clarity by the aerial camera lens than those images near the edge of the picture. A clearer and sharper image is also created by a ground object that is sharply defined with respect to its surrounding background. Obviously such high-quality images can be identified and measured with greater accuracy (smaller σ standard error) on the comparator. If some of the ground objects are especially marked prior to the photography, it is logical to expect very small standard errors of comparator measurement for their images and to want to weight their observation equations heavily in the least square solution.

As discussed in previous chapters, if one equation is to be favored W times more strongly than other equations, then this equation should be entered W times into the set of observation equations before forming the normal equations. The concept of weighting can be introduced by means of a weight matrix W defined as a diagonal matrix whose diagonal elements are the number of times the particular equation is to be entered in the set of equations.

It is shown in statistics that the weight matrix is a function of the standard error of the observations. Then the weight matrix is:

$$W = \begin{bmatrix} 1/\sigma_1^2 & & 0 \\ & \ddots & \\ 0 & & 1/\sigma_n^2 \end{bmatrix}$$

(assuming independent observations)

where σ^2 is the square of the standard error (variance) of the observation. In practice it is only the relative size of the diagonal elements that is important.

Since a high-quality image is observed on a comparator with a small σ standard error, its weight $1/\sigma^2$ is correspondingly higher.

The weight matrix can be entered into the computations by forming the normal equations according to the equation $A^TWAx_o=A^TWl$. The same effect can also be obtained by multiplying each observation equation by $1/\sigma$ which is the square root of the corresponding diagonal element in the W weight matrix. See APPLIED METHOD OF LEAST SQUARES. This latter technique is used in the Coast and Geodetic Survey programs.

OBSERVATION EQUATION MULTIPLIERS

Computing the σ for the images observed on the comparator is not practical because only 3 to 5 measurements are made on an image. Also, the computation of σ for every image on every plate in the block would be a tedious operation. For this reason, the Coast and Geodetic Survey has developed emperical values for the $1/\sigma$ equation multipliers based on experience.

The equation multiplier is applied to the observation equation in two separate steps:

1. Image Location: A multiplier is applied so as to weight the observation equations written for an image on the basis of camera lens resolution. Thus the location of the image on the plate is used to determine the value of the multiplier. At the C and GS, images within 0.07 meters of the principal point are given a weight of 1.0. Optional weights can then be applied for images at other plate locations. Thus images lying between 0.07 meters and 0.12 meters from the principal point have a somewhat smaller weight while images further away carry a still smaller weight value. These optional weights can range from 0.1 through 1.0.

2. Target Identification: A multiplier is applied so as to weight the observation equations for an image that depends on the definition of the target object with respect to its surrounding backround. The control station objects are usually pre-marked prior to photography to insure exact identification of their images on the photographs. Their equations are obviously more reliable than the equations written for pass-point objects which usually are not pre-marked. The multiplier for equations provided for those objects that are NOT pre-marked is automatically set at 1. The multiplier for equations from pre-marked objects can range from 1 through 99 in the C and GS programs. Usually the multiplier for the pre-marked objects does not exceed 5.

THE NORMAL EQUATION MATRIX

After weighting the observation equations for image quality, the block camera orientation phase proceeds to the formation of the normal equations. A typical system of normal equations for block adjustment is shown in Figure 1 where each line contains the coefficients for one normal equation. The solid portions represent the presence of non-zero numbers and the open areas above the main diagonal consist entirely of zeros. The terms to the left of the diagonal are not shown since they are equal to corresponding terms above the diagonal because the normal equation matrix is symmetrical.

The 3-by-3 "stairsteps" shown at Z1 represent coefficients for the three dX dY dZ correction terms to be computed for the provisional X Y Z object coordinates. The 6-by-6 "stairsteps" at Z3 refer to the dw dφ dk dXo dYo dZo correction terms to be computed and added to the initial approximations of the camera parameters determined in the space resection phase. The column at Z2 represents the list of constant terms in the normal equations. The solid portions at Z are the intermediate cross-products of the normal equation formation procedure. Although the

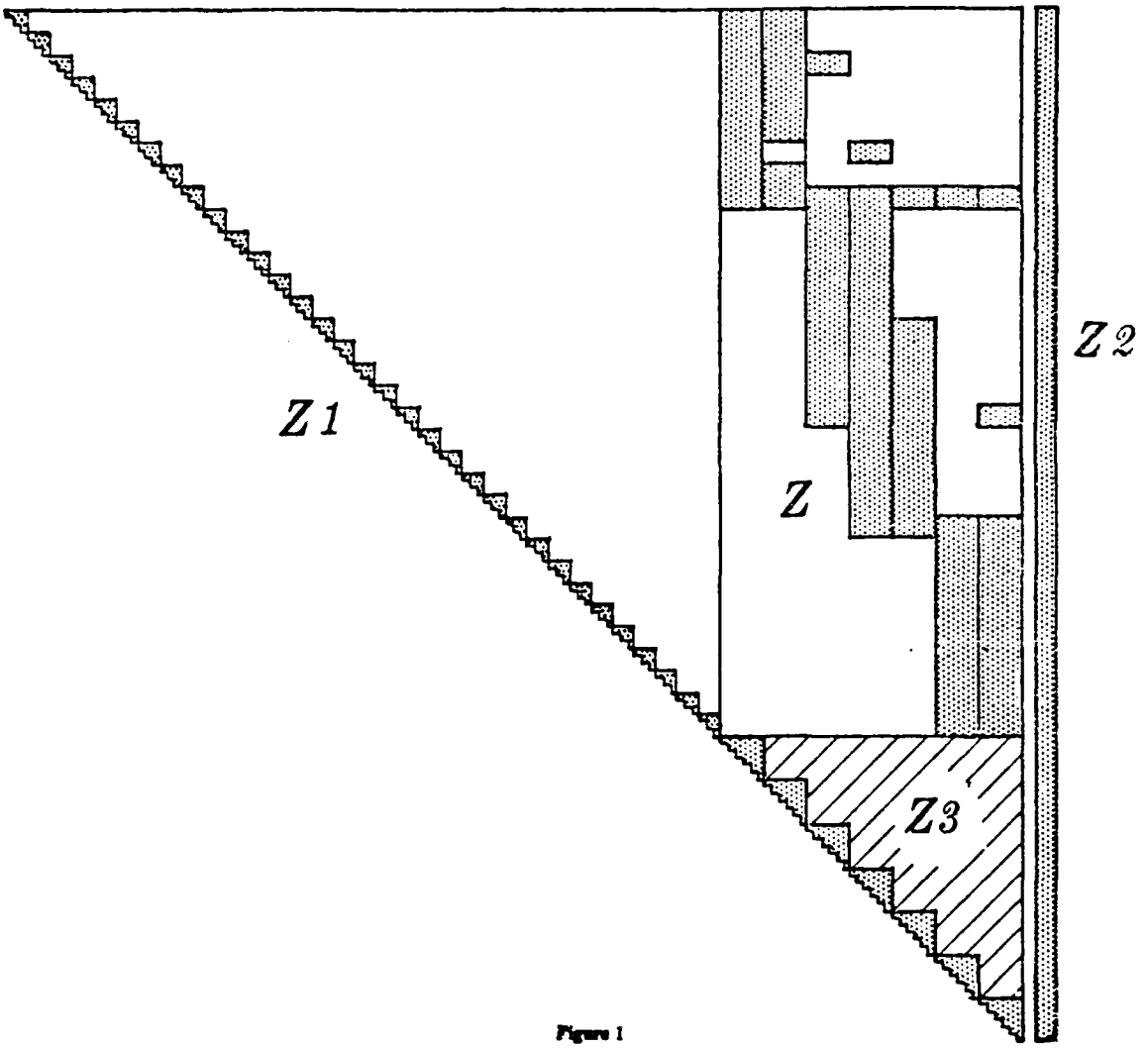

Figure 1

submatrix of camera parameters shown at Z3 contains blocks of zeros in the cross-hatched area during the formation of normal equations, large portions of the cross-hatched area become non-zero during the solution of the equations. It is the solution of this submatrix that requires the predominant heavy burden of arithmetic operations.

STORAGE OF THE NORMAL EQUATIONS

The number of unknowns present in the solution of a large block of photographs can be huge. For example, a 200-photo block may contain as many as 1500 pass-point objects and control stations (200x6 pass-points per photo = 1200 pass-point objects and perhaps 300 control stations) thereby providing 4,500 dX dY dZ unknowns. In addition there would be 1200 dw dφ dk dXo dYo dZo camera parameter correction terms (200x6 parameters per photo). Thus there may be 5,700 unknowns present in the normal equations. A conventional storage of a 5700-by-5701 normal equation matrix would require over 32 million words of computer memory. By taking advantage of the large blocks of zeros whose positions in the matrix are fixed by the nature of the photogrammetric problem, this storage can be reduced to less than one million words of memory. A solution of this size is feasible on either the IBM 7030 (STRETCH) computer which has a combined core and disk memory exceeding 1.5 million words, or on the CDC 6600 computer with a combined core and auxiliary disk memory approaching 17,000,000 words.

The use of disk memory is significant as regards computer time and costs. Since the computations take place using data stored in core memory, it is necessary to transfer the contents of several large arrays from core to disk storage thereby leaving the core arrays free to hold new information. As the computations progress, data will move from core storage to disk storage and back again hundreds of times depending on the number of photographs in the block. The actual transfer of data between disk and core is extremely rapid, but locating the reading heads to the desired disk address is relatively slow (disk being a random access device) thus materially increasing the time of computer operation.

To accomplish this large solution, the normal equation matrix is divided into the four irregular submatrices Z, Z1, Z2, and Z3 shown in Figure 1 and stored in the computer. Only the solid sections are stored for Z, Z1, and Z2 thereby eliminating the zero portions of the matrix. However, storage area must be provided for both the solid portion and the cross-hatched area of Z3 because of the non-zero numbers that are generated in this section during the solution of the normal equations. This type of compression technique obviously demands a strict "housekeeping" program procedure to keep track of all the elements comprising the normal equation matrix.

WEIGHTING THE CONTROL STATIONS IN THE SOLUTION

The two linearized collinearity observation equations are arranged so as to explicitly minimize the v_x and v_y residual observational discrepancies in the x and y refined image coordinates. As previously noted, these two equations are written for every image on every photograph in the block created by the pass-point objects and the control stations. When they are written for the images created by the control station objects it is necessary to recognize that the initial approximations of X Y Z are really obtained by observations during the ground surveying operations of triangulation and traverse. Thus dx dy and dX dY dZ are observed parameters and dw dφ dk dXo dYo dZo are true parameters in these equations. See chapter LEAST SQUARE MINIMIZATION OF COMBINATIONS OF OBSERVATIONAL ERRORS..

Since the observed parameters -dx and -dy are explicitly minimized in the linearized collinearity equations, we must write extra constraint equations for the remaining dX dY dZ observed parameters and add them to the set of observation equations before forming the normal equations. The extra equations are of the form $v_{dX}=dX-0$ $v_{dY}=dY-0$ $v_{dZ}=dZ-0$ where dX dY dZ are the observed corrections found by solving the normal equations and 0 is the true value for these terms if the X Y Z field observations are exactly correct. The v_{dX} and v_{dY} equations are written for horizontal control stations while the v_{dZ} equation is written for the vertical control stations. All three equations are written for stations that are both horizontal and vertical control.

Weights are then applied so that these extra constraint equations will be favored during the formation and solution of the normal equations. Forming the normal equations causes these weights to become added to the main diagonal elements which are the coefficients of the unknown dX dY and/or dZ parameters. When the normal equations are solved, these weights cause a reduction in the magnitude of the dX dY and/or dZ corrections required for the initial approximations of X Y Z as given by the field observations. Thus the extra equations and their weights constrain the least square block adjustment in favor of the ground observations.

The present C and GS block adjustment program weights the solution in favor of the control stations by increasing the size of the appropiate main diagonal terms before solving the normal equations. However this program provides for the multiplication of the main diagonal term by an empirical number instead of adding on a number. The effect is essentially the same in enforcing the known X Y Z of the control stations. These empirical position weights usually range between 2 and 4 in practice.

Note that a position weight of infinity would yield a zero dX dY and/or dZ on solution. This is equivalent to deleting the dX dY and/or dZ correction terms from the observation equations. The problem would then be one of resection.

SOLUTION OF THE NORMAL EQUATIONS

The solution of the normal equations is accomplished at the C and GS by a Gauss-Cholesky elimination method. A description of this method is given on the last two pages of this chapter. The product of the forward and back solution consists of the corrections to all the camera parameters and the initial ground coordinates of the pass-point objects and control stations.

In applying the computed incremental corrections for use in the following iteration of the problem, the P_{11} and P_{21} constant terms should be recomputed using the updated true parameters and the original observations for the observed variables. The other P-coefficients should be recomputed using updated true parameters and updated observations. For the pass-points, this means recomputing P_{11} and P_{21} using updated w ϕ k Xo Yo Zo X Y Z values and the original refined $\underline{x}$ and $\underline{y}$ image coordinates. The coefficients $P_{12}...P_{17}$ $P_{22}...P_{27}$ should use the updated values of w ϕ k Xo Yo Zo X Y Z x y. In the case of the control stations, however, the P_{11} and P_{21} constant terms should use updated w ϕ k Xo Yo Zo values together with the original refined $\underline{x}$ and $\underline{y}$ image coordinates and field observed X Y Z coordinates. The coefficients $P_{12}...P_{17}$ $P_{22}...P_{27}$ should use updated w ϕ k Xo Yo Zo X Y Z x y values.

The C and GS experience has been that the good data furnished by the preliminary analytic programs makes it unnecessary to iterate the block adjustment computation. In other words, the computed dw dϕ dk corrections to the camera parameters are usually sufficiently close to the 0.00001 radian value in the very first pass that we can terminate the solution. A second pass would yield only negligible changes in the answers to the camera parameters and ground coordinates. For this reason, the present C and GS analytic programs do not provide for updating the observations in computing the P-coefficients. If a second pass is necessary, however, the space-resection phase is by-passed on the repeated solution.

It had been suggested that large systems of equations treated by the Gauss-Cholesky elimination method might not result in a satisfactory solution because of the rounding off of numbers arising from repeated multiplications. This difficulty was found not to be significant for several reasons. The solution determines only relatively small corrections to data which are already fairly accurate. Each repetition or iteration is based on a new set of coefficients which, in turn, are based on the corrected values of the parameters. Experience has shown the average size of the corrections on any iteration to be from one-tenth to one-thousandth of the magnitude on the previous iteration. Consequently, such

a system will continue to converge rapidly as long as the leading one or two significant digits of the corrections remain undamaged by the encroachment of round-off discrepancies. The floating arithmetic and 14 to 15-digit word-length on the computers make this possible. Similar solutions in the adjustments of very large networks in classical geodesy have always been satisfactory. Finally, no difficulties have been encountered in block adjustment solutions involving as many as 180 photographs.

OUTPUT FROM THE BLOCK CAMERA ORIENTATION PHASE

The output from the orientation phase of the C and GS program consists of: (1) the maximum angular correction required by each program pass; (2) the finalized ground coordinates of all the relative orientation pass-point objects; (3) the field observed ground coordinates of the weighted control stations; (4) the misfit of the block solution to these weighted control stations; (5) the residual observational discrepancies of all images on each photograph and the RMS-value for the entire block; (6) the sines and cosines of the final three orientation angles of each photograph; and (7) the final three linear coordinates of each camera station.

OBJECT-INTERSECTION PHASE

All of the pass-points and weighted control stations contribute equations to the normal equation matrix and thus influence the least square orientation solution. The unweighted control stations may also be allowed to contribute equations to the orientation solution as if they are pass-points. However, there may exist other objects in the block which, for some reason, are undesirable for use in the orientation solution. Their refined image coordinates and the finalized camera parameters form the orientation solution can be used to compute their ground coordinates by the Iterative Intersection Method previously discussed. In addition the weighted control stations can also be computed as if they were pass-points by processing them through this Iterative Intersection Method. In this method, the residual observational discrepancies v_x and v_y are minimized according to the principles of least squares.

Because the ground X Y Z of the object are the only unknowns, the original collinearity equations (17) and (18) can be arranged to provide the following observation equations:

$$\begin{bmatrix} v_x = (P_{15}X+P_{16}Y+P_{17}Z-P_{15}Xo-P_{16}Yo-P_{17}Zo)/A_3B \\ v_y = (P_{25}X+P_{26}Y+P_{27}Z-P_{25}Xo-P_{26}Yo-P_{27}Zo)/A_3B \end{bmatrix}$$

These equations are written for each plate on which the object appears. Least squares is applied to obtain a solution for X Y Z minimizing the residual image discrepancies. The computation is iterated until the change in X and Y does not exceed one micron on the smallest-scale photograph in the block. The maximum residual image discrepancy is determined and its magnitude evaluated. If it is excessive, the image is discarded and the object intersection solution is repeated using the remaining images. The ground coordinates of an unlimited number of objects may be determined in this manner.

The completion of the object intersection phase concludes the block adjustment program. If secant plane coordinates were used in the block adjustment computations, the adjusted X Y Z secant plane coordinates are transformed back into the original ground coordinate system by applying the secant plane transformation program in its inverse mode.


DAT
FILM